# A general circulation model study of the global carbonaceous aerosol distribution

W. F. Cooke[1]
Nicholas School of the Environment and Earth Sciences, Duke University, Durham, North Carolina, USA

V. Ramaswamy
Geophysical Fluid Dynamics Laboratory, Princeton, New Jersey, USA

P. Kasibhatla
Nicholas School of the Environment and Earth Sciences, Duke University, Durham, North Carolina, USA

Received 4 August 2000; revised 23 July 2001; accepted 2 August 2001; published 17 August 2002.

[1] Atmospheric distributions of carbonaceous aerosols are simulated using the Geophysical Fluid Dynamics Laboratory SKYHI general circulation model (GCM) (latitude-longitude resolution of $\sim 3^\circ \times 3.6^\circ$). A number of systematic analyses are conducted to investigate the seasonal and interannual variability of the concentrations at specific locations and to investigate the sensitivity of the distributions to various physical parameters. Comparisons are made with several observational data sets. At four specific sites (Mace Head, Mauna Loa, Sable Island, and Bondville) the monthly mean measurements of surface concentrations of black carbon made over several years reveal that the model simulation registers successes as well as failures. Comparisons are also made with averages of measurements made over varying time periods, segregated by geography and rural/remote locations. Generally, the mean measured remote surface concentrations exceed those simulated. Notwithstanding the large variability in measurements and model simulations, the simulations of both black and organic carbon tend to be within about a factor of 2 at a majority of the sites. There are major challenges in conducting comparisons with measurements due to inadequate sampling at some sites, the generally short length of the observational record, and different methods used for estimating the black and organic carbon amounts. The interannual variability in the model and in the few such measurements available points to the need for doing multiyear modeling and to the necessity of comparing with long-term measurements. There are very few altitude profile measurements; notwithstanding the large uncertainties, the present comparisons suggest an overestimation by the model in the free troposphere. The global column burdens of black and organic carbon in the present standard model integration are lower than in previous studies and thus could be regarded as approximately bracketing a lower end of the simulated anthropogenic burden due to these classes of aerosols, based on the current understanding of the carbonaceous aerosol cycle. Of the physical factors examined, the intensity and frequency of precipitation events are critical in governing the column burdens. Biases in the frequency of precipitation are likely the single biggest cause of discrepancies between simulation and observations. This parameter is available from very few sites and thus lacks a comprehensive global data set, unlike, say, monthly mean precipitation. Several multiyear GCM integrations have been performed to evaluate the sensitivity of the global mean black carbon distribution to the principal aerosol parameters, with due regard to variability and statistical significance. The most sensitive parameters, in order of importance, turn out to be the wet deposition, transformation from hydrophobic to hydrophilic state, and the partitioning of the emitted aerosol between the hydrophobic and hydrophilic varieties. From the sensitivity tests, it is estimated that the variations of the global mean column burden and lifetime of black carbon are within

[1]Also at Geophysical Fluid Dynamics Laboratory, Princeton, New Jersey, USA.


0148-0227/02/2001JD001274$09.00

about a factor of 2 about their respective standard values. The studies also show that the column burdens over remote regions appear to be most sensitive to changes in each parameter, reiterating the importance of measurements in those locations for a proper evaluation of model simulation of these aerosols. *INDEX TERMS:* 0305 Atmospheric Composition and Structure: Aerosols and particles (0345, 4801); 0345 Atmospheric Composition and Structure: Pollution—urban and regional (0305); 0365 Atmospheric Composition and Structure: Troposphere—composition and chemistry; *KEYWORDS:* carbonaceous aerosol, sensitivity studies, aerosol scavenging

## 1. Introduction

[2] There is concern about the changing composition of the atmosphere due to anthropogenic emissions. A consequence of the combustion of fossil fuel is the emission of carbonaceous aerosol. This carbonaceous aerosol can be broken into two fractions, an organic carbon (OC) fraction that may be reactive in the atmosphere and a nonreactive black carbon (BC) fraction. The optical properties of these two fractions are also quite dissimilar. The organic fraction has optical properties that mainly involve scattering in the visible spectrum. The BC aerosol is, as its name suggests, highly absorbing in the solar spectrum and is the only ubiquitous anthropogenic aerosol with a significant absorption cross section. The abundance of OC as a fraction of the carbonaceous aerosol may differ significantly due to the combustion process and fuel type. The ratio BC:OC may not be constant in the atmosphere, due to differing lifetimes and sources, and *Penner et al.* [1995] have shown, with a simple box model, that the radiative forcing of the atmosphere is quite sensitive to the ratio of BC to OC emission.

[3] While the majority of modeling efforts have concentrated on the sulfur cycle, it is also necessary to calculate the global mass distribution of carbonaceous aerosol in order to provide a better picture of the impact of anthropogenic emissions on the atmosphere and the impacts on radiative transfer thereof. Recent studies and experiments have found that the OC mass concentration in both anthropogenically influenced source and remote areas may be of the same magnitude as that of sulfate [*Cachier et al.*, 1990; *Novakov and Corrigan*, 1996; *Hegg et al.*, 1997].

[4] While previous studies [*Cooke and Wilson*, 1996; *Liousse et al.*, 1996; *Cooke et al.*, 1999] have calculated the global distribution of the carbonaceous aerosol, this work examines more comprehensively the sensitivity of the carbonaceous aerosol burden to different parameters governing its distribution. For example, the solubility properties of the aerosol determine the amount of the aerosol that remains in the atmosphere and therefore determine the radiative impact of this aerosol type. By varying the different parameters responsible for the carbonaceous aerosol concentration in a three-dimensional (3-D) general circulation model (GCM), we estimate the variability of the atmospheric burden of the aerosol in this study. We also compare the simulated aerosol concentrations with observational data now available. Section 2 discusses the implementation of the carbonaceous aerosol sources in a GCM. Section 3 discusses the model-observation comparison. Section 4 presents the results from the sensitivity studies, while section 5 comprises the conclusions.

## 2. Implementation of Carbonaceous Aerosols in SKYHI

### 2.1. Meteorological Model

[5] The model used in this work is the Geophysical Fluid Dynamics Laboratory 3-D SKYHI model, which was originally developed from the latitude-longitude, sigma coordinate GCM described by *Holloway and Manabe* [1971] and updated by *Fels et al.* [1980], *Mahlman et al.* [1994], and *Hamilton et al.* [1995]. The SKYHI model uses a 40-level hybrid vertical coordinate, which is terrain following near the ground, merging into pure isobaric coordinates above 321 hPa, with the highest model level occurring at the 0.01-hPa level. A detailed description of a basic version of the model is given by *Hamilton et al.* [1995]. The model resolution used in this work is the N30 version ($\sim 3^\circ$ latitude $\times$ $3.6^\circ$ longitude).

[6] The shortwave radiative transfer algorithm in the SKYHI GCM follows *Lacis and Hansen* [1974], as modified by *Ramaswamy and Friedenreich* [1992] to accurately account for water vapor absorption at small path lengths. The infrared radiative algorithm of the GCM has been described by *Schwarzkopf and Fels* [1991]. In the algorithm version used here, $H_2O$, $CO_2$, and $O_3$ are the only radiatively active gases that are considered. A more detailed discussion of the radiation transfer code in the SKYHI GCM is given by *Schwarzkopf and Ramaswamy* [1999]. Clouds are predicted according to the model of *Wetherald and Manabe* [1988]. The clouds predicted in this manner [*Ramachandran et al.*, 2000] are included in the radiative transfer calculations of the model. However, in this study, aerosols do not interact with radiation.

[7] The aerosol transport scheme used in this work is that of *Lin and Rood* [1996] using the positive-definite piecewise parabolic method. This constrains the diffusivity of the subgrid distribution so that it prevents the generation of negatives. This is necessary as the gradients in the aerosol distribution are strong enough that the transport scheme could introduce negative concentrations. For vertical mixing, the stability of the column is compared to the moist adiabat and convective activity is initiated when the Richardson number is $<0.25$.

[8] The precipitation scheme used in this model produces moist and dry convective adjustment at the end of each time step. When the relative humidity of the grid box exceeds 100%, the excess water vapor is condensed and removed in a precipitation event.

[9] All model results discussed here are 3-year integrations, initialized from a 30-year unforced run. A spin-up period of 3 months is allowed after the aerosols have been introduced in the model. However, as 3 years does not appear to be long enough for the aerosol to reach equili-

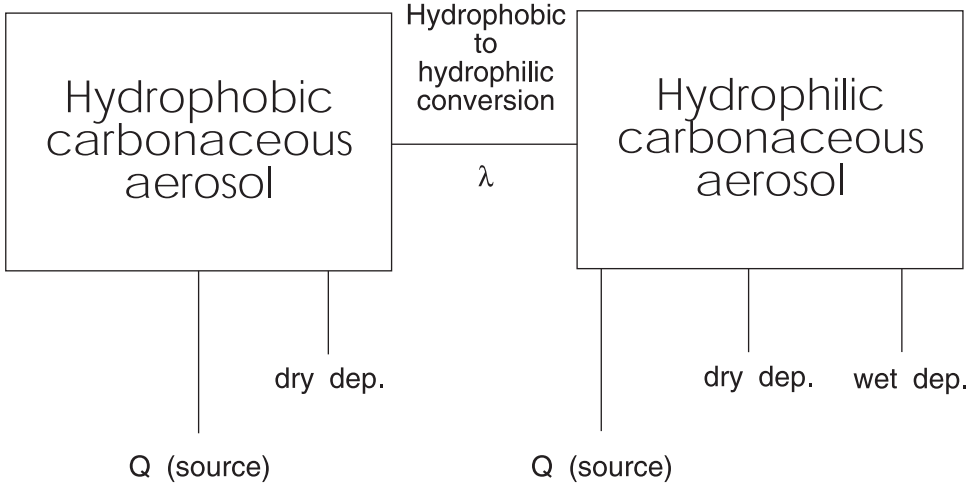


**Figure 1.** Emission and transformation scheme for carbonaceous aerosol as implemented in the general circulation model.

brium in the stratosphere, the discussions here are restricted to altitudes below 200 hPa.

### 2.2. Implementation of Carbonaceous Aerosol in SKYHI

[10] The emissions of carbonaceous aerosol have been taken from *Cooke et al.* [1999] and were transformed from a $1° \times 1°$ resolution grid to the N30 resolution ($\sim 3.6° \times 3°$) by allocating the appropriate fraction of each emission grid cell to the appropriate N30 resolution SKYHI grid cell. It should be noted here that the emissions are for fossil fuel only and total 5.1 Tg for BC and 14 Tg for OC. The submicron OC emissions derived by *Cooke et al.* [1999] were for primary emissions and have been doubled as suggested in that work in order to allow for secondary production of OC aerosol within the grid box of the source region.

[11] The aerosol module used to model the carbonaceous aerosol is based on that used for carbonaceous particles by *Cooke and Wilson* [1996] and *Cooke et al.* [1999]. The scheme is shown in Figure 1.

[12] Particulate carbon is predominantly hydrophobic, but a certain fraction of the emissions may be hydrophilic [*Cachier*, 1998]. BC and OC both have various compounds attached to the surface [*Smith et al.*, 1989] that may determine their atmospheric behavior and also allow a chemical change in the properties of the surface layer as it ages in the atmosphere. Emissions of BC are assumed to be 80% hydrophobic, while the emissions of OC are assumed to be 50% hydrophobic. The aging process for both BC and OC is represented by a transfer of hydrophobic to hydrophilic aerosol with an exponential lifetime of 1.15 days, which provided the best model-to-measurement fit in the Model of the Global Universal Tracer Transport in the Atmosphere (MOGUNTIA) model [*Cooke and Wilson*, 1996]. The aerosol lifetime is assumed to be governed by wet and dry deposition, and no chemical sinks are used in this work. Wet deposition of the hydrophilic aerosol assumes that all of the aerosol affected by precipitation is removed. The fraction of the aerosol removed in each grid box is identical to the areal fraction of the grid box that is precipitating. The total precipitation within a model column is calculated as described above and is assumed to be due to standard convective or stratus clouds, which have liquid water contents (LWC) of 2 and 0.5 g $m^{-3}$, respectively. The areal fraction of the grid column affected by precipitation is then calculated as

$$A = \frac{P(g\ m^{-2})}{L(g\ m^{-3}) \times dz(m)}\ , \qquad (1)$$

where $A$ is the areal fraction, $P$ is precipitation, $L$ is LWC, and $dz$ is the depth of the precipitating cloud [*Balkanski*, 1991]. The same fraction of aerosol is then removed in each precipitating layer. In this model the scavenging of aerosol is the same for frozen and liquid precipitation. Below-cloud scavenging is not included. The dry deposition flux to the ground is assumed to be proportional to both the concentration in the lowest model layer and to a prescribed dry deposition velocity. For hydrophilic carbonaceous aerosol this is assumed to be 0.025 cm $s^{-1}$ over land and 0.1 cm $s^{-1}$ over ocean [*Ganzeveld et al.*, 1998]. Hydrophobic aerosols are deposited by a constant velocity of 0.025 cm $s^{-1}$ as the hydrophobic aerosols are assumed not to be influenced by wetted surfaces. These parameters have been used previously by *Cooke et al.* [1999] and in this work will be called the "standard" model. As part of the sensitivity tests, the parameters discussed above are subsequently varied, and the resulting impact on the burdens and surface concentrations is investigated.

## 3. Comparison of the Carbonaceous Model With Measured Data

[13] After implementing the submicron emission fields of *Cooke et al.* [1999] a model spin-up period of 3 months was allowed. The model was then run for a further 3 years, and monthly means over this 3-year period are compared with measurements in sections 3.13.23.3–3.4. The annual average atmospheric burden and lifetimes of the carbonaceous aerosols are given in Table 1 and can be compared with those of previous works. The lifetimes found here, calcu-

**Table 1.** Atmospheric Burdens and Lifetimes of Carbonaceous Aerosol[a]

| Species | Emissions, Tg | Burden, days | Lifetime, days |
|---|---|---|---|
| BC (this work) | 5.1 | 0.060 | 4.29 |
| BC (FF, C99) | 5.1 | 0.073 | 5.29 |
| BC (FF, L96) | 6.64 | 0.070 | 3.86 |
| BC (FF, CW96) | 7.96 | 0.17 | 7.85 |
| OC (this work) | 14.0 | 0.130 | 3.39 |
| OC (FF, C99) | 7.0 | 0.087 | 4.54 |
| OC (FF, L96) | 21.9 | 0.232 | 3.86 |

[a]Data sources are C99, *Cooke et al.* [1999]; CW96, *Cooke and Wilson* [1996]; L96, *Liousse et al.* [1996]. OC is organic carbon. FF is the fossil fuel component of the burden assuming, where necessary, that the lifetime of black carbon (BC) from fossil fuel and biomass burning are identical.

lated as the mean annual global burden divided by the annual emission, are typical for fine atmospheric hydrophilic particles, with the lifetime of OC being similar to that of another radiatively important aerosol, sulfate.

[14] The BC burden found here is ~18% lower than that found by *Cooke et al.* [1999], even though the emission sources of aerosol are identical. This implies that the scavenging process removes more aerosol in the SKYHI model, and this is likely due to the wet deposition process in the model. The burden found here is also lower than that of *Liousse et al.* [1996], but in this case the lifetime of the aerosol is longer, implying that the scavenging process in the work of *Liousse et al.* [1996] is even more efficient than in this work. The burden of *Cooke and Wilson* [1996] (0.17 Tg BC due to fossil fuel BC) is much higher. This is due to the emission scheme used in this work, which emits less hydrophobic aerosol and thus shortens the lifetime of the aerosol, and is also due to the lower total emissions used here.

[15] The OC burden can be compared to that of *Cooke et al.* [1999] and *Liousse et al.* [1996]. The difference in the burdens between this work and that of *Cooke et al.* [1999] can partially be attributed to the doubling of the emissions in this work, but the aerosol is also scavenged more quickly, as can be seen from the shorter lifetime. The burden of OC found by *Liousse et al.* [1996] is estimated by assuming that the lifetimes of BC and OC are identical in that work. The difference between the present work and that of *Liousse et al.* [1996] can be attributed to the ratio of the emissions between the two works, although it would appear that the scavenging in this scheme is also slightly more efficient, as evidenced by the shorter lifetime. The difference in lifetimes of OC and BC in this work demonstrates the important effect due to the partitioning of the emissions between the hydrophobic and hydrophilic fractions.

### 3.1. Variability of Concentrations on Different Timescales

[16] It is instructive to consider the simulated variability in the concentration of the aerosol when sampled over different time periods. Modeled daily mean concentrations of BC from the mid-North Atlantic (36°N–45°N, 45.0°W–55.8°W) were used to construct a set of weekly and monthly mean concentrations. The geometric mean and deviations of these data sets were then calculated. When going from monthly to daily averages, the geometric mean remains the same, but the geometric deviation increases. For the data compiled in this way, the geometric mean was 11.4 ng $m^{-3}$ with geometric deviations of 1.98, 2.72, and 4.32 for the monthly, weekly, and daily data, respectively. A quantitatively similar pattern is seen in the Climate Monitoring and Diagnostics Laboratory (CMDL) measurements. Therefore, when comparing, say, monthly mean modeled BC concentrations with measured quantities, a certain amount of bias could arise due to the differences in sampling periods. For example, the short-term point and vertical distribution measurements, discussed in sections 3.2.2 and 3.2.3, are generally made over periods of several hours to several days and, as seen above, may lead to measured averages that may be significantly different from the true mean concentration due to the small number of samples and thus the higher probability of a larger deviation. The reduction in variability for longer sampling periods is not surprising, as the mean for the longer periods is an average over the shorter time periods. Further, from the probability distribution of the daily samples, the probability of sampling concentrations near the long-term mean is higher. For example, the probability of a daily sample having a concentration of 10 ng $m^{-3}$ is ~3 times that of having a concentration of 100 ng $m^{-3}$. Therefore a hypothetical monthly mean could contain 23 samples of 10 ng $m^{-3}$ and 8 samples of 100 ng $m^{-3}$. The geometric monthly mean would be 18 ng $m^{-3}$, a value much closer to 10 ng $m^{-3}$ than to 100 ng $m^{-3}$. There is much less variability in the column burden, however. For the same area the column burden is 0.137 mg $m^{-2}$ with geometric deviations of 1.90, 1.99, and 2.21 for the monthly, weekly, and daily data, respectively.

### 3.2. Comparison of Modeled Concentrations of BC With Measurements

[17] We will now make a comparison between the modeled and measured values of BC at various sites around the globe. We will only make comparisons with measurements made in the Northern Hemisphere, as this is where the majority (94% of the inventory) of fossil fuel emissions occur. The evaluation of the model comprises a comparison of modeled concentrations of BC in both air and precipitation with those measured.

#### 3.2.1. Comparison of Average of Measurements and Model of BC for Long-Term Sites

[18] The model monthly geometric means are calculated for the 3-year run. These are compared to the geometric mean and the range or deviation of the measured data.

[19] The CMDL operates a continuous light-absorption photometer at various sites that can be used to infer daily BC concentrations. The measurements of absorption have been converted to surface concentrations using a factor of 9.3 $m^2$ $g^{-1}$ [*Haywood and Ramaswamy*, 1998]. One such site is Sable Island, Nova Scotia (60°W, 43.9°N), where measurements have taken place since October 1995. The monthly geometric mean and interannual monthly geometric deviation of the observed and monthly modeled concentrations are shown in Figure 2.

[20] For the first 5 months of the year the modeled values are approximately half of those measured. There is somewhat better agreement during the summertime, although the model still underpredicts the concentrations. The best agreement is in the final 3 months of the year, where eight of the

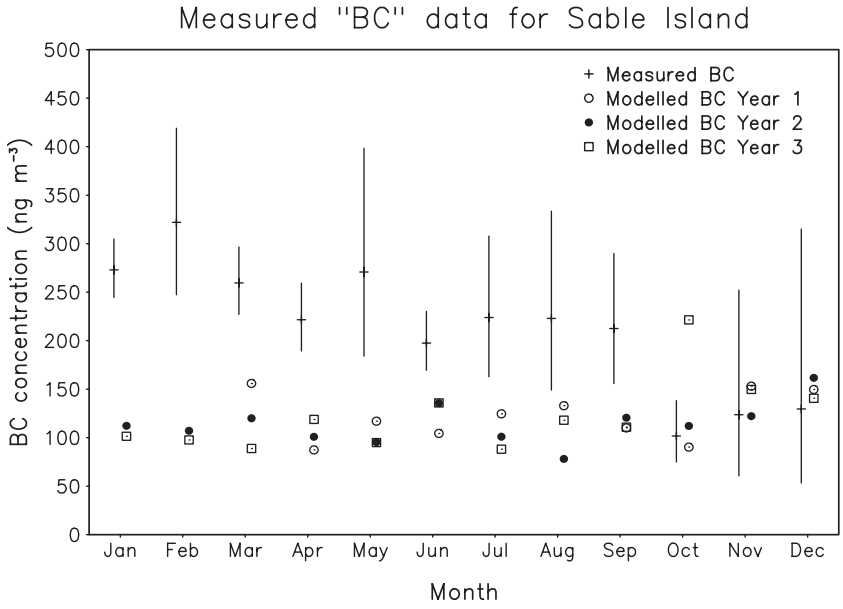


**Figure 2.** Comparison of modeled (3 years of data) and measured black carbon (BC) at Sable Island (60°W, 43.9°N). Mean and geometric deviation of the observations is shown, while, for the model, the values for each of the 3 years of simulation are plotted.

nine modeled monthly mean concentrations are close to the measured mean concentrations. The disagreement in the first few months may imply that the emissions upwind of Sable Island are too low or that the modeled scavenging of the aerosol is too efficient.

[21] Some insight on whether the emissions are too low may be obtained by looking at the modeled and measured BC concentrations at Bondville, Illinois (88.4°W, 40.1°N). Bondville is located on the western edge of a large areal emission source, so if the emissions are generally too low in the model, it would underestimate the concentration of the aerosol at this site. However, if the modeled concentrations are reasonable at Bondville, this implies that rather than a bias in the emissions, it is likely that the removal processes for the aerosol in the transit between the source region and Sable Island are too efficient. The monthly mean concentrations for Bondville are shown in Figure 3. In this case the observations and modeled BC are in quite good agreement for the first 3 months and are underestimated during the summer period to the same degree as at Sable Island. The peak in the measured concentrations in October may be due to interference from dust from farming practices affecting the observational estimate (J. Ogren, personal communication, 1999). The reasonable agreement between the model and measured concentrations throughout the year and the possible interference of absorbing dust suggest that the

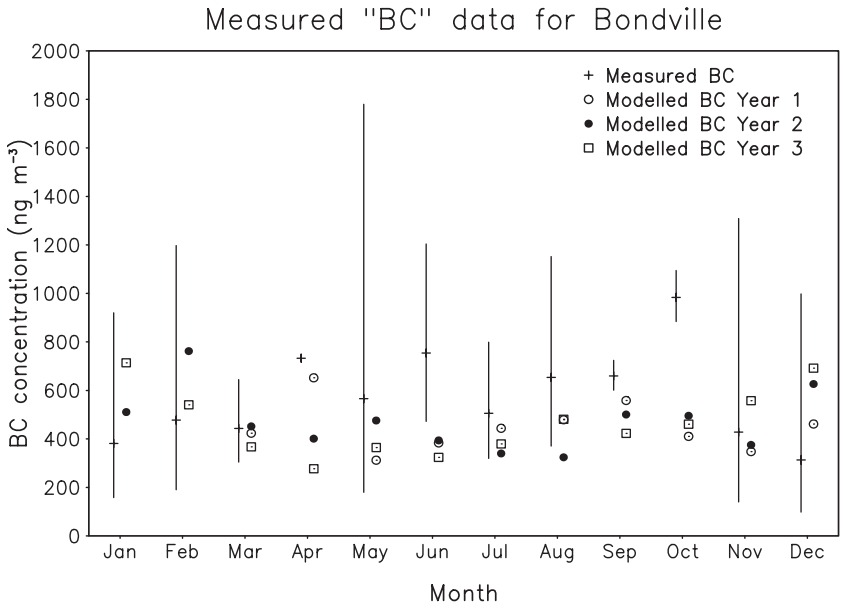


**Figure 3.** Same as Figure 2 except at Bondville (88.4°W, 40.1°N).

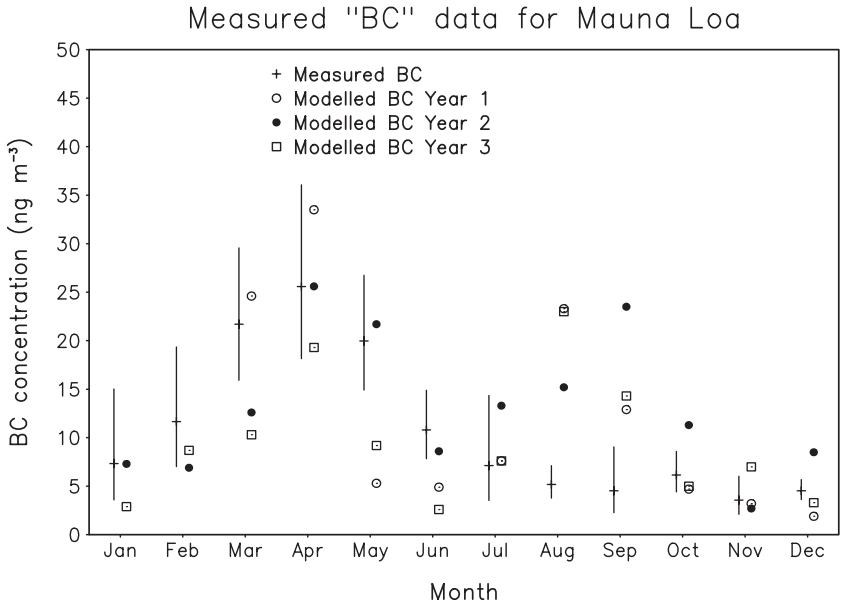


**Figure 4.** Same as Figure 2 except at Mauna Loa (155.6°W, 19.5°N, 3397 m above sea level (asl)).

emission of BC is not seriously underestimated in this region. Also, on the basis of comparison with precipitation data, we know that the frequency of precipitation is overestimated in the region near Sable Island. This is likely the biggest source of discrepancy between the model and observations. A secondary factor could be a bias in the emissions. Thus the underestimation of the model in predicting BC concentrations at Sable Island is a discrepancy more likely due to the scavenging process.

[22] Measurements of light absorption have also been performed at the free tropospheric site of Mauna Loa, Hawaii (155.6°W, 19.5°N, 3397 m above sea level (asl)). These are presented in Figure 4 and generally show an underestimation in the modeled concentrations in the first 6 months of the year. However, the peak concentration in April is reproduced very well.

[23] There is a secondary peak in the modeled concentrations in August that is not seen in the measurements. Isentropic back-trajectory analysis for this month as derived from the SKYHI model and as supplied by CMDL, shown in Figure 5, shows that both sets of trajectories have an easterly bias, with the bias being much more pronounced in the SKYHI case. The easterlies are much stronger in the SKYHI case, implying that BC from Central America is contributing to the secondary modeled peak in concentrations.

[24] A 7-year average of the measurements from the data of *Cooke et al.* [1997] for BC measurements at Mace Head, Ireland (9.85°W, 53.3°N), have been used to compare with the model. The comparison between the sector modeled and measured values of BC mass concentrations are shown in Figure 6, in which the monthly measured and modeled means are for air masses where the wind direction was from the marine sector (180°–300°).

[25] There is an underestimation in the modeled concentrations in the first half of the year, with better agreement in the second half of the year. In August and September the model strongly overestimates the concentrations of BC at Mace Head during one of the model years. This is due to strong transport off the European continent that is then transported back to Mace Head on westerly winds. The general underestimation of the model suggests that too much aerosol is scavenged in this instance as well. The lack of seasonality in the modeled concentrations is probably due to the lack of seasonality of the emissions but also may point to a deficiency in the seasonality of the precipitation simulation.

[26] Long-term measurements of BC tend to be inferred from absorption measurements using a constant absorption cross section. However, *Liousse et al.* [1993] found that the absorption cross section of BC varied by a factor of 4 as one moves from source to remote regions. This variation may cause some problems in evaluating the actual BC mass concentrations, especially at remote sites. It should also be remembered that there are inherent difficulties in the measurement of BC or light absorption coefficients [*Heintzenberg et al.*, 1997], which may account for some of the discrepancies seen in the comparison.

### 3.2.2. Comparison of Point Measurements of BC

[27] There have been many measurements of BC for time periods of several days to several years. The sites where these measurements have been made are shown in Figure 7. The boxed areas are the regions where comparisons of the modeled and measured data are given in Figure 8. These measurements have been made with a variety of methods, and it is difficult to ascertain how representative or accurate the measurements really are of the actual regional concentrations of BC. The measurements for the United States are mainly derived from the Interagency Monitoring of Protected Visual Environments (IMPROVE) network [*Malm et al.*, 1994]. These measurements are made at a variety of stations, mainly situated in national parks. The variability obtained from the available measurement record, as well as the variability obtained from the model simulation for the grid box corresponding to the measurement site and for the appropriate time period of the measurement, is

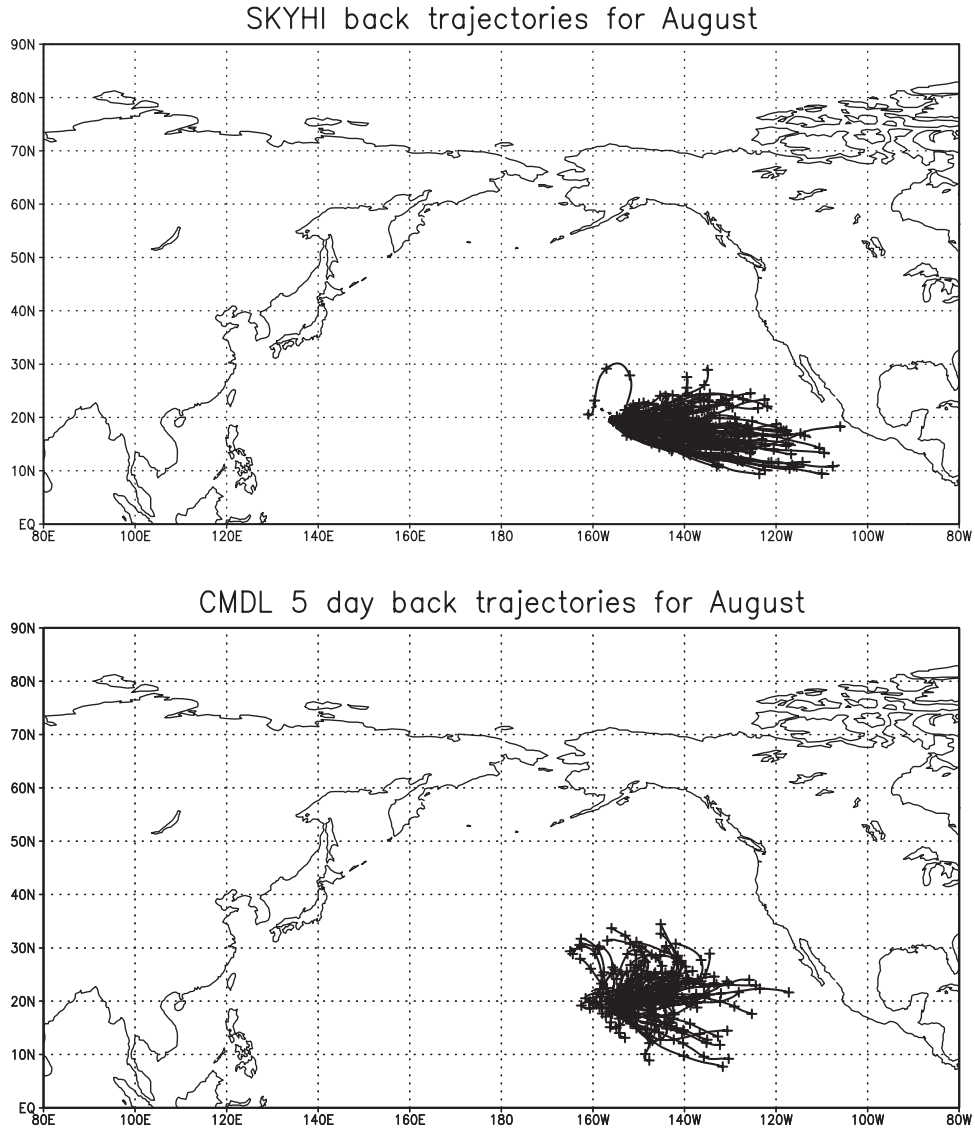


**Figure 5.** Comparison of (top) 5-day SKYHI and (bottom) Climate Monitoring and Diagnostics Laboratory isentropic back-trajectories to Mauna Loa in August.

plotted in Figure 8. All three model years of the model simulation are considered.

[28] In Figure 8a a comparison of modeled and measured BC concentrations in the southwestern United States is presented. There is good agreement between the model and the measurements in this region. The greatest discrepancy is for the site at Saint Nicholas Island (site 1) [*Hidy et al.*, 1974]. Saint Nicholas Island is just offshore of Los Angeles and may therefore be heavily influenced by this large source area. In Figure 8b a comparison is shown for the northeastern United States. In this case the model tends to overpredict the concentration of BC at a number of sites but, at 8 of the 13 sites, by less than a factor of 2.

[29] In Figure 8c the modeled concentrations of BC are compared with various measurements made in western Europe. Here Europe is arbitrarily divided at longitude 10.5°E. In this case the model appears to underpredict the concentration of BC. For measurements made in western Portugal (site 2) the model underestimates the measurements by at least an order of magnitude. This may be due to the steep gradient in the model concentration fields in this area. However, the good agreement at Corsica (site 3) and Landes (site 4), an island and a coastal site, may mean that a source of BC is missing in the area of Portugal where the sampling took place. At Jungfraujoch (site 1), at a height of 3573 m asl, the gradient in the vertical may be partly responsible for some of the discrepancy seen.

[30] In Figure 8d the modeled concentrations of BC are compared with various measurements made in Europe east of 10.5°E. The ranges of the model and observations are quite large, and the model is within the range of the observations in four of the five cases.

[31] In Figure 8e a comparison between modeled and measured concentrations is made for eastern Asia. There is a large scatter in the data, although a reasonable comparison can be seen for a couple of the sites. The site with the best agreement is on the mainland of China, while the rest of the measurements are made on islands, which may account for

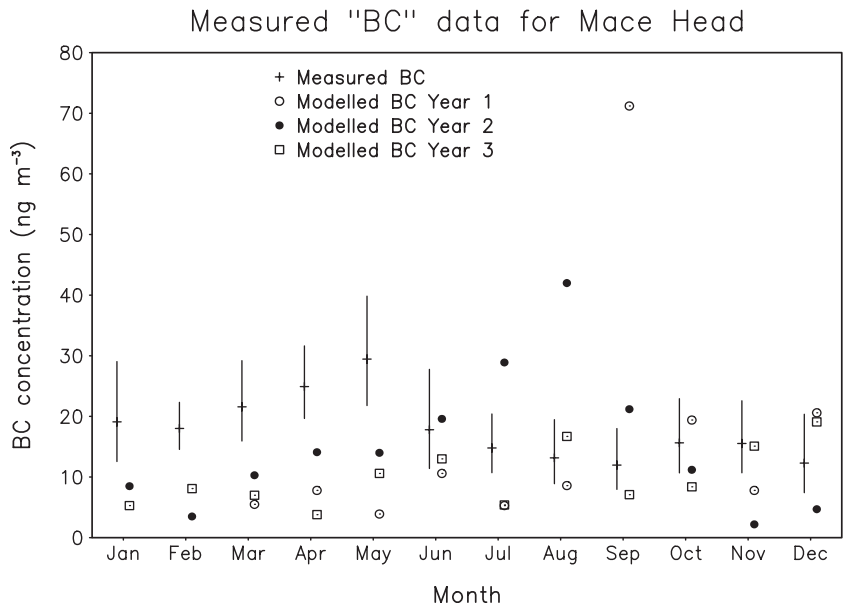


**Figure 6.** Comparison of modeled (3 years of data) and measured BC at Mace Head (9.85°W, 53.3°N) for the marine sector.

some of the discrepancies since the gradient in the model concentrations may contribute to some uncertainty in the model concentrations.

[32] In Figure 8f a comparison is made between modeled and measured concentrations for sites at other locations around the globe. In this case the model underestimates the concentration of BC at 8 of the 10 sites compared. The greatest discrepancy is at the lowest modeled concentrations of BC, which are in the most remote areas, and this comparison can lead to one of two conclusions. The model may be

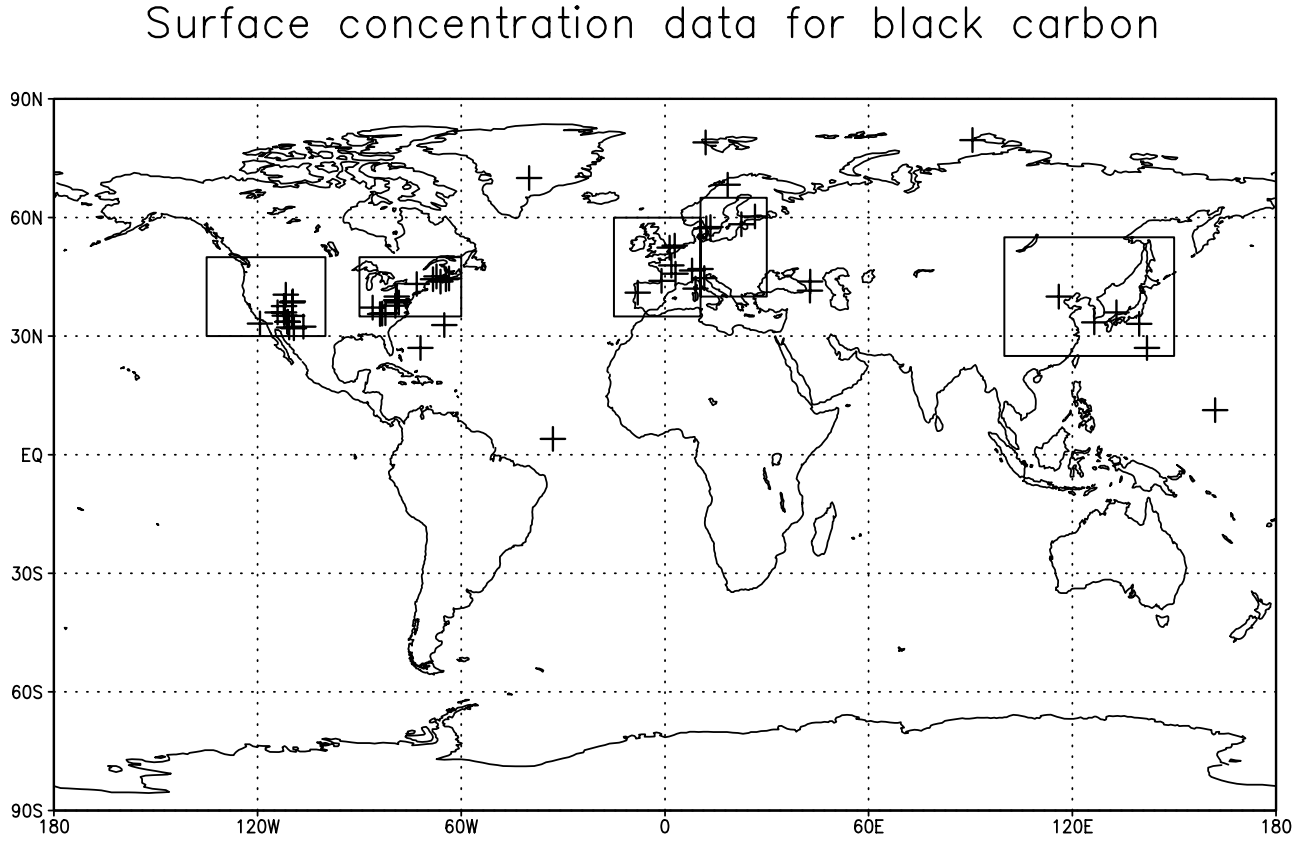


**Figure 7.** Sites where short-term measurements of BC have been made at the surface. Enclosed areas show the regional breakdown of sites as discussed in Figure 8.

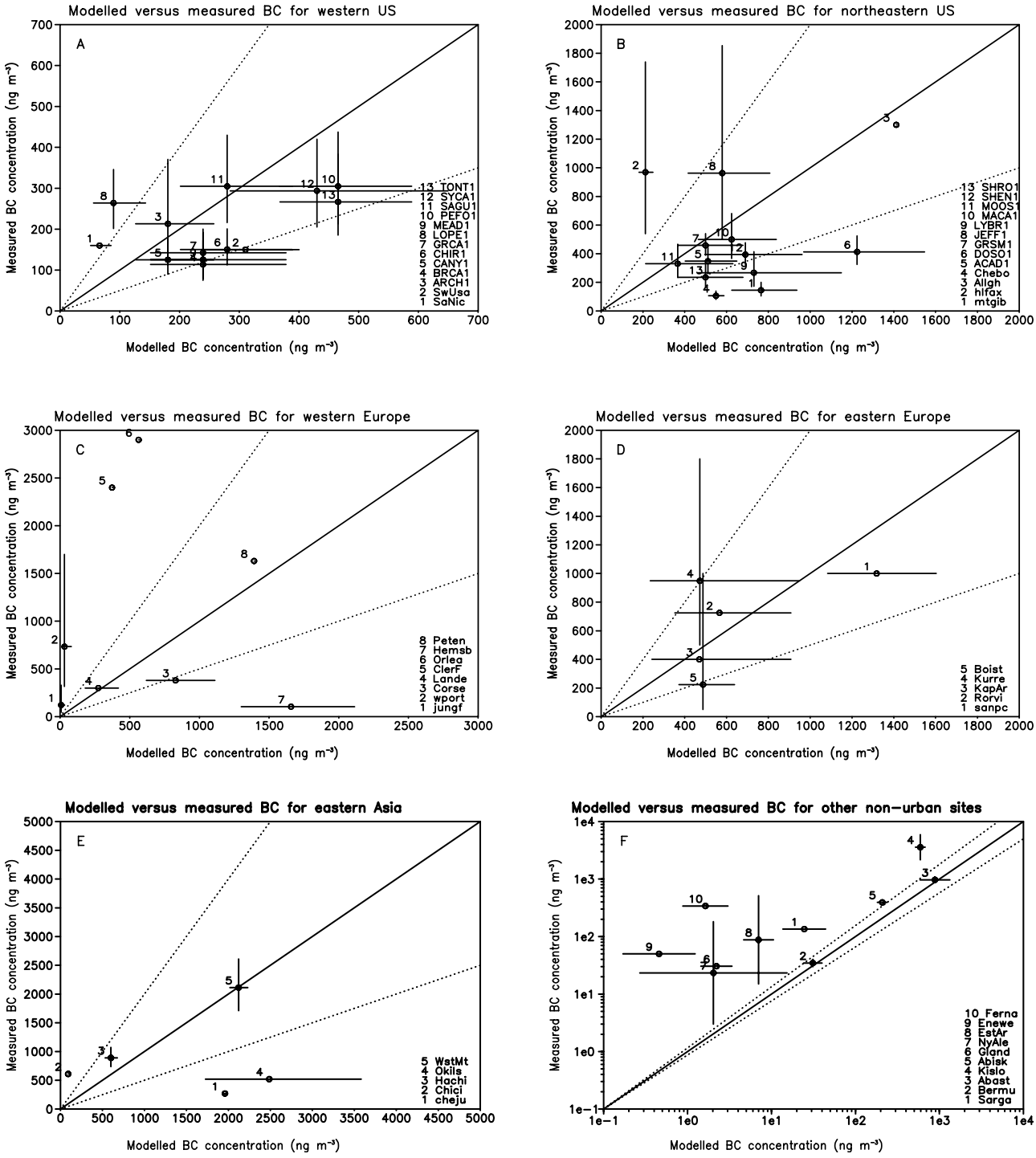


**Figure 8.** Comparison of modeled and measured BC at various sites. Horizontal and vertical bars denote the variability in the modeled and available measured concentrations, respectively. Dotted lines indicate a range of a factor of 2. Acronyms for the sites are explained in Appendix A. A 1 *Hidy et al.* [1974], 2 *Pinnick et al.* [1993], 3–13 *Malm et al.* [1994], B 1 *Bahrmann and Saxena* [1998], 2 *Keeler et al.* [1990], 3 *Chýlek et al.* [1996], 4–13 *Malm et al.* [1994], C 1 *Lavanchy et al.* [1999], 2 *Castro et al.* [1999], 3–4 *Cachier et al.* [1989a], 5 *Cachier et al.* [1990] D 1–3 *Zappoli et al.* [1999], 4 *Brorström-Lundén et al.* [1994] 5 *Raunemaa et al.* [1993], E 1 *Kim et al.* [1999], 2,4 *Ohta and Okita* [1984], 3,6 *Parungo et al.* [1994], 5 *Mukai et al.* [1990], F 1,9 *Andreae et al.* [1984], 2 *Wolff et al.* [1986], 3 *Lyubovtseva and Yatskovich* [1989], 4 *Noone and Clarke* [1988], 5 *Pertuisot* [1997], 6 *Heintzenberg* [1982], 7 *Polissar* [1993], 8 *Cachier et al.* [1990].

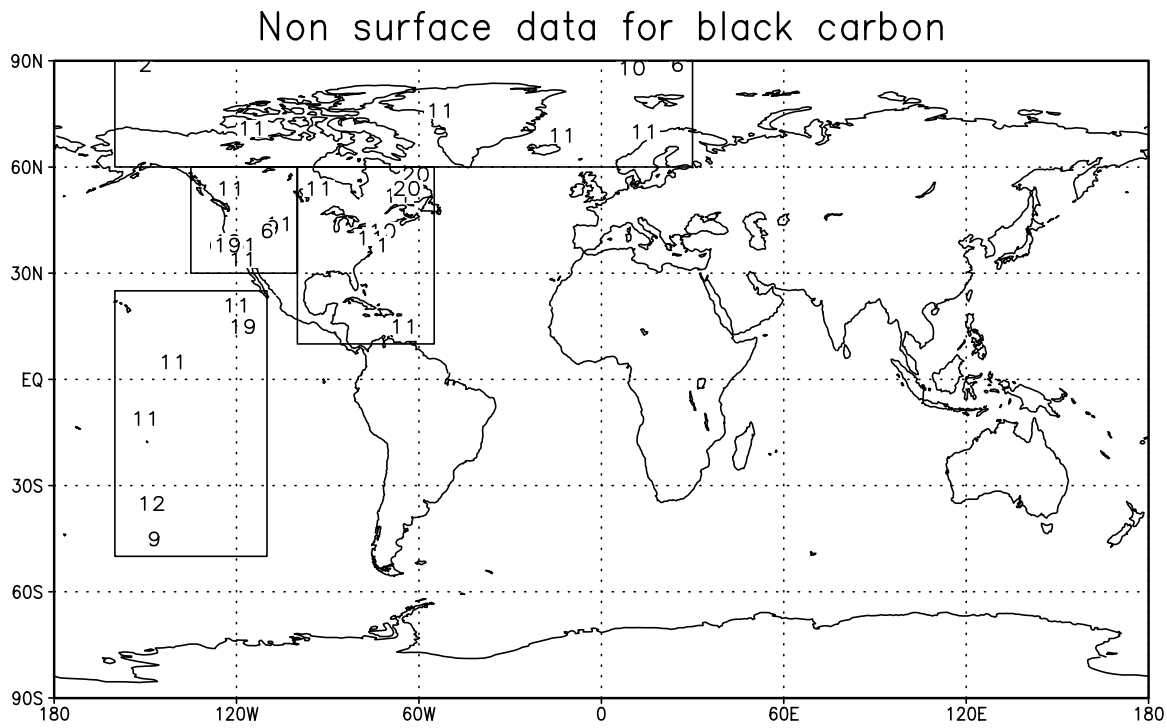


**Figure 9.** Points where measurements of BC have been made. Numbers represent height (km asl). These heights and the enclosed areas are used to segregate the data shown in Figure 10.

underestimating the BC concentration in remote regions or the measurements may be reaching the detection limit of the instrument used. Another possibility for the measurements made at Enewetak (site 9) and Fernando do Noronha (site 10) is that BC from biomass burning is being measured at these sites. Biomass burning emissions are not included in this work, so comparison with measurements in tropical regions may be affected by biomass burning emissions.

[33] A short run (3 months of spin-up plus 12 months) of the model was performed with biomass burning sources (5.98 Tg BC and 36 Tg OC, from the biomass burning BC emission of *Cooke and Wilson* [1996] and the ratio of ~6 for OC:BC in the biomass burning inventory of *Liousse et al.* [1996]) included. At the sites where comparisons were made, the BC air concentrations are hardly affected. At the only site with a major impact from biomass burning (Fernando do Noronha, site 10 in Figure 8f), the BC concentration was increased by an order of magnitude (from 1 to 10 ng $m^{-3}$). Therefore biomass burning is not the explanation for the discrepancies seen here. Overall, although there is a large variability in the measurements and model results, the simulated values are within about a factor of 2 of the observations at most of the sites.

### 3.2.3. Comparison of Measurements and Model in the Vertical Profile

[34] Figure 9 shows regions examined in Figure 10. Figure 10 presents a comparison between the data of *Hansen and Novakov* [1988], *Pueschel et al.* [1992], and *Blake and Kato* [1995] and the model for nonsurface measurements of BC. The data from these sources are samples from aircraft, so by their very nature they are extremely short-term period measurements. The measured data are segregated by height and over the regions shown in Figure 9. The modeled concentrations at the appropriate locations and heights are segregated in the same manner. In three of the four regions shown here the model overestimates the concentration of BC by a factor of 2 or more and, in some cases, by more than an order of magnitude. However, the variability in measurements can itself exceed an order of magnitude, which acts as a constraint to perform rigorous quantitative comparisons. In most cases the ranges of the measured and modeled concentrations overlap each other. Over the eastern United States the model predicts BC concentrations that are in good agreement with measurements for altitudes below 16 km; above this altitude the model underpredicts the measured values. Overall, it would appear that there is too much BC in the model's upper troposphere, a problem that has been noticed previously in other models [*Cooke and Wilson*, 1996; *Liousse et al.*, 1996; *Cooke et al.*, 1999].

### 3.2.4. Comparison of Wet Deposition of BC

[35] Wet deposition is the most efficient sink for submicron aerosol in the atmosphere. A comparison of the modeled and measured wet deposition of BC is made in Table 2a.

[36] In general, the model tends to be at the lower end of the range of the measurements of wet deposition of BC, with the greatest discrepancies being in the Arctic region. This is likely due to the weak transport of aerosols to this region. The wet deposition is underestimated to a much lesser degree in the less remote regions (<72°N). One possible explanation for being at the lower end of the measured range is that the modeled values are averages over daily means for three separate years, while the observations are typically from a campaign of a few months. A comparison of the observations for April from Abisko

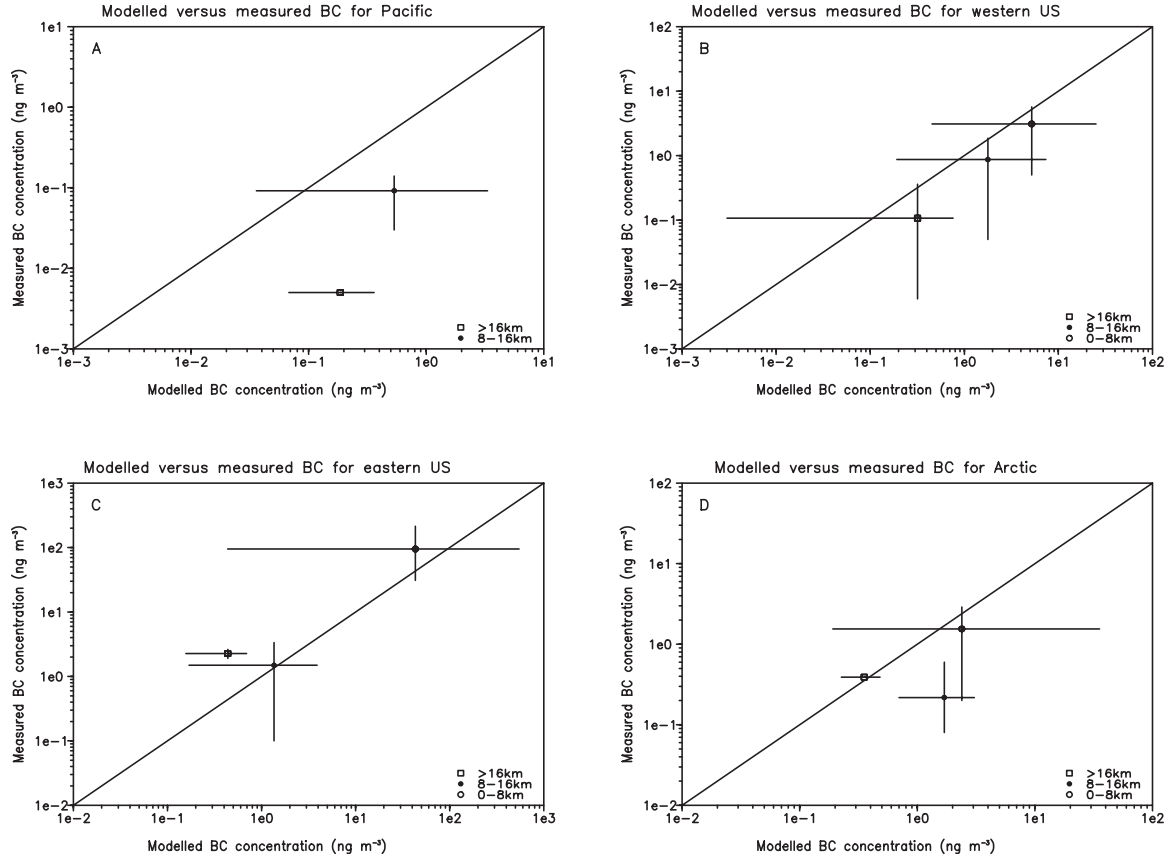


**Figure 10.** Comparison of modeled and measured vertical distribution of BC in various regions. Horizontal and vertical bars denote the range of the modeled and measured concentrations, respectively.

(10.2–36.6 μg $L^{-1}$) [*Clarke and Noone*, 1985] and northern Sweden (100–500 μg $L^{-1}$) [*Ogren et al.*, 1984] shows the interannual variability of the wet deposition as well as possible discrepancies between measurement methods. The comparison of wet deposition in Nova Scotia, along with the underestimation of BC concentration in air at Sable Island, reinforces the idea that the aerosol is being scavenged too quickly in this area of the globe.

[37] We also report the flux of BC to the surface due to wet deposition in Table 2b for three sites. Comparison of the

**Table 2a.** Comparison of Modeled and Measured Wet Deposition of BC in SKYHI[a]

| | | | | Wet Deposition, μg $L^{-1}$ | |
|---|---|---|---|---|---|
| Station Name | Latitude | Longitude | Time Period | Modeled | Measured |
| Alert | 82°30′N | 62°30′W | Nov–Dec 1983 | 1.7–3.5 | 45.5 (0–127)[b] |
| Greenland Sea | 79°48′N | 4°12′W | July 1983 | 4.3 | 38.7 (5.4–75.5)[b] |
| Spitzbergen | 79°N | 12°E | May 1983 | 5.3 | 31 (6.7–52)[b] |
| Summit | 72°N | 38°5′W | Annual | 4.8 | 5.4, 3.0[c,d] |
| Barrow | 71°18′N | 156°36′W | March–April 1983 | 6.2–8.4 | 23 (7.3–60.4)[b] |
| Abisko | 68°18′N | 18°30′E | March–April 1984 | 35.9–94.5 | 33 (8.8–77)[b] |
| Northern Sweden | 66°N | 20°E | April–Aug 1981 | 17.2–94.5 | 172 (30–700)[e] |
| Southern Sweden | 60°N | 16°E | April–Aug 1981 | 47.8–115.1 | 193 (20–600)[e] |
| Mace Head | 53°18′N | 9°54′W | Oct–Nov 1989 | 5.3–16.7 | 31 (9–94)[f] |
| Gif sur Yvette | 49° | 2°E | 1988–1990 | 125 | 333 (27–1348)[f] |
| Porspoder | 48°30′N | 4°46′W | March 1994 | 32.4 | 31[c] |
| Hurricane Hill | 48°N | 123°30′W | April 1984 | 12.7 | 14.7 (10.1–18.5)[b] |
| Seattle | 47°36′N | 122°18′W | Dec 1980–Jan 1981 | 44.7–55.5 | 60 (28–130)[e] |
| Halifax | 44°38′N | 63°35′W | Jan–May 1995 | 34.1–52.9 | 2.6–6.3[g] |
| Bridgewater, Nova Scotia | 44°25′N | 64°31′W | Jan–Sept 1995 | 34.1–66.4 | 0.5–8.2[g] |

[a]Range in the modeled values is the range of the monthly modeled means for the same period as the measurements.
[b]*Clarke and Noone* [1985].
[c]*Pertuisot* [1997].
[d]*Masclet et al.* [2000].
[e]*Ogren et al.* [1984].
[f]*Ducret and Cachier* [1992].
[g]*Chýlek et al.* [1999].

**Table 2b.** Comparison of Modeled and Measured Wet Deposition Flux of BC in SKYHI[a]

| Station Name | Latitude | Longitude | Time Period | Wet Deposition, μg m$^{-2}$ month$^{-1}$ | |
|---|---|---|---|---|---|
| | | | | Modeled | Measured[b] |
| Northern Sweden | 66°N | 20°E | April–Aug 1981 | 1015–2766 | 4000–6000 |
| Southern Sweden | 60°N | 16°E | April–Aug 1981 | 2299–7198 | 5000–11000 |
| Seattle | 47°36′N | 122°18′W | Dec 1980–Jan 1981 | 1890–2045 | 648–9576 |

[a]Range in the modeled values is the range of the monthly modeled means for the same period as the measurements.
[b]*Ogren et al.* [1984].

agreement between the model and measured values for rainwater concentrations and the flux of BC at each site allows us to conclude that the total precipitation is reasonably well represented in the three cases shown, as the ratio of modeled and measured fluxes is similar to that for the rainwater concentrations. The underestimation of the wet deposition of BC suggests that the model should have a higher global burden than the other studies, which is in contradiction to what is seen in Table 1. An explanation for this is that the wet deposition measurements are biased toward the Arctic region, where the burden in this study is low. A comparison with *Cooke and Wilson* [1996] and *Liousse et al.* [1996] of the surface distribution of BC (not shown here) demonstrates that the aerosol concentration in the Arctic region is lower in this study by perhaps an order of magnitude. However, while 50% of the annual mean global BC burden is present between 30°N and 60°N, only 5% is present between 60°N and 90°N. Therefore any underestimation of the aerosol burden in the Arctic is not likely to have a large effect on the global aerosol burden. The SKYHI model additionally overpredicts the precipitation in the Arctic in the western hemisphere by a factor of 2 (the absolute values are, however, small), which leads to a diminution of the already low concentrations in the Arctic.

[38] It should also be noted here that for the biomass burning emission run described earlier, the wet deposition of BC did not change appreciably for the sites included in this study. From this run, the wet deposition of BC from biomass burning sources was ∼10% of the wet deposition due to fossil fuel.

### 3.3. Comparison of Modeled Concentrations of Organic Carbon With Measurements

[39] It is very difficult, considerably more so than in the case of BC, to compare the modeled mass concentrations of OC from fossil fuel sources with measurements. This is partly due to the fact that there are other sources of OC aerosol. There are natural sources of aerosol organic substances as well as secondary production of aerosol from gaseous emissions from natural and anthropogenic sources. Observational data are even more sparse for OC than for BC, and there are few long-term measurements.

#### 3.3.1. Comparison of Point Measurements of OC

[40] The sites where point measurements of OC have been made are shown in Figure 11. The boxed areas are the regions where a comparison of the modeled and measured data is made in Figure 12. Again, the variability in both the measured and simulated values is considered.

[41] In Figure 12a a comparison of the OC concentrations is made for the western United States. In this case the model tends to underestimate the concentration of OC in all cases. In fact, the measured concentrations show only a factor of 2 variation, while the modeled concentrations vary by an order of magnitude for different sites. A possible explanation of the discrepancies found here is that other sources of OC are available, such as biomass burning organics or natural sources of OC aerosol. These other sources are not provided for in this model, so an underestimation of the concentration of aerosol is likely in areas where fossil fuel OC is not predominant. However, from a short model run with biomass burning emissions, we see no great influence on OC concentrations at the sites we compare in this study.

[42] In Figure 12b a comparison is made for the eastern United States. In this case, there is greater variability in the measured estimates. The model also underestimates the concentration of OC in this region, although the variabilities of the model and measured values overlap to the extent that one can claim reasonable agreement between the model and measurements. In this case it would appear that the sources of OC in the northeastern United States are dominated by fossil fuel emissions.

[43] In Figure 12c the modeled and measured OC concentrations are compared for western Europe. Again, the model underestimates the concentration of OC. The greatest underestimation is in western Portugal (site 1), which is similar to the comparison with BC (compare Figure 8c). The best agreement is for the measurements made at Corsica (site 2) and Landes (site 3). At Corsica and Landes the measurements are certainly rural and are probably representative of the regional concentrations of OC.

[44] In Figure 12d a comparison is made for measurements and modeled concentrations of OC for eastern Europe. The lack of data points prohibits the drawing of any conclusive evidence of agreement or otherwise in this area.

[45] In Figure 12e the measured and modeled OC concentrations are compared for eastern Asia. There is reasonable agreement for most of the sites here. The best agreement is for the island sites of Cheju, Korea (site 1), and Hachijo-jima, Japan (site 3). The good agreement for these sites probably means that the overestimation of the concentrations at Oki Island (site 4) is not an indication that the emissions in this region are too high. At the more remote site of Chichi-jima, Japan (site 2), the model underestimates the concentration of OC, but there may be some influence of natural sources.

[46] In Figure 12f a comparison is made between OC measured and modeled concentrations for sites in nonurban regions of the globe other than those discussed above. The disagreement between the model and measurements increases as one moves farther from the source regions. At Abastumani, Georgia (site 3), the agreement is best, and as one moves to more remote areas, there is greater disagreement. The greatest disagreement is at the tropical

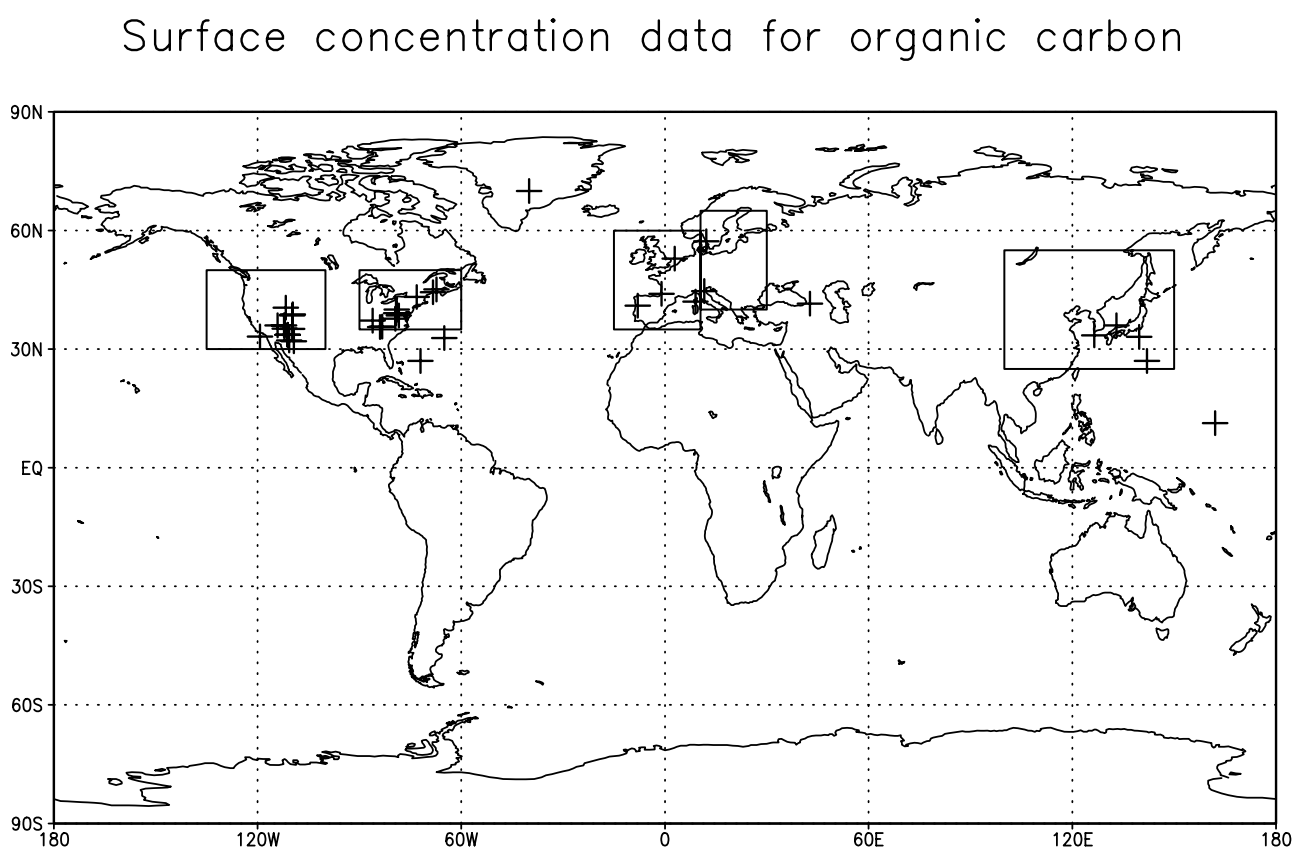


**Figure 11.** Sites where short-term measurements of organic carbon (OC) have been made at the surface. Enclosed areas show the regional breakdown of sites as discussed in Figure 12.

site of Enewetak (site 5). This is also the site that is most remote from the influence of fossil fuel usage. If one extrapolates the agreement between the model and measured concentrations to where the model predicts that the concentrations should be 0.1 ng $m^{-3}$, i.e., practically nonexistent, the measurements show a background concentration of several hundred nanograms per cubic meter. This background concentration could be contributed by either natural or biomass burning sources of OC.

[47] In light of the short model run with biomass burning sources described earlier, natural sources of OC appear to be the likely contributor in the regions where we compare model calculations with observations. Again, in an overall sense, and considering the large variability in the measurements, the simulated results are within about a factor of 2 of observations at several sites.

### 3.3.2. Comparison of Wet Deposition of OC

[48] There are few measurements of wet deposition of OC. One must be careful when comparing measurements of OC deposition, as most measurements are of the total OC contained in the precipitation. This includes not only the particulate OC but also dissolved organic carbon (DOC) from the adsorption of gaseous organic compounds. In fact, the DOC component of the organic carbon is the main component. The situation is further complicated by the dissolution of OC aerosol once it has been introduced into cloud or rain drops. This has the effect of reducing the observed particulate OC content and should lead to an overestimation by the model of the wet deposition of OC aerosol when compared with observations. This reduction of OC in the particulate phase in precipitation may be on the order of 20% [*Ducret and Cachier*, 1992]. A summary of measurements of wet deposition of OC is presented in Table 3.

[49] Considering the difficulties in measuring the wet deposition of OC, as mentioned above, the model is in excellent agreement with the observations. The only site where a factor of 2 difference is seen is at Gif-sur-Yvette, which is in a source region and is likely to be underestimated. However, the number of sites where comparison is made is insufficient to draw any firm conclusions about the global accuracy of the wet removal of OC. This could be aided by a greater number of measurement campaigns.

### 3.4. Comparison of Modeled Precipitation With Observations

[50] Although the underestimation of concentrations of BC and OC might imply that the scavenging process is too strong, the comparison of measured and modeled wet deposition data shows that the wet deposition in the model is comparable to that measured in nature. The lowest latitude at which the wet deposition of carbonaceous aerosol has been measured is 44°N. Sampling of wet deposition at lower latitudes is necessary since several large source regions are at lower latitudes. The flux of carbon to the surface is dependent on four parameters, namely, the tracer concentration in the air, the frequency and intensity of the precipitation, and the vertical distribution of the formation of the precipitation.

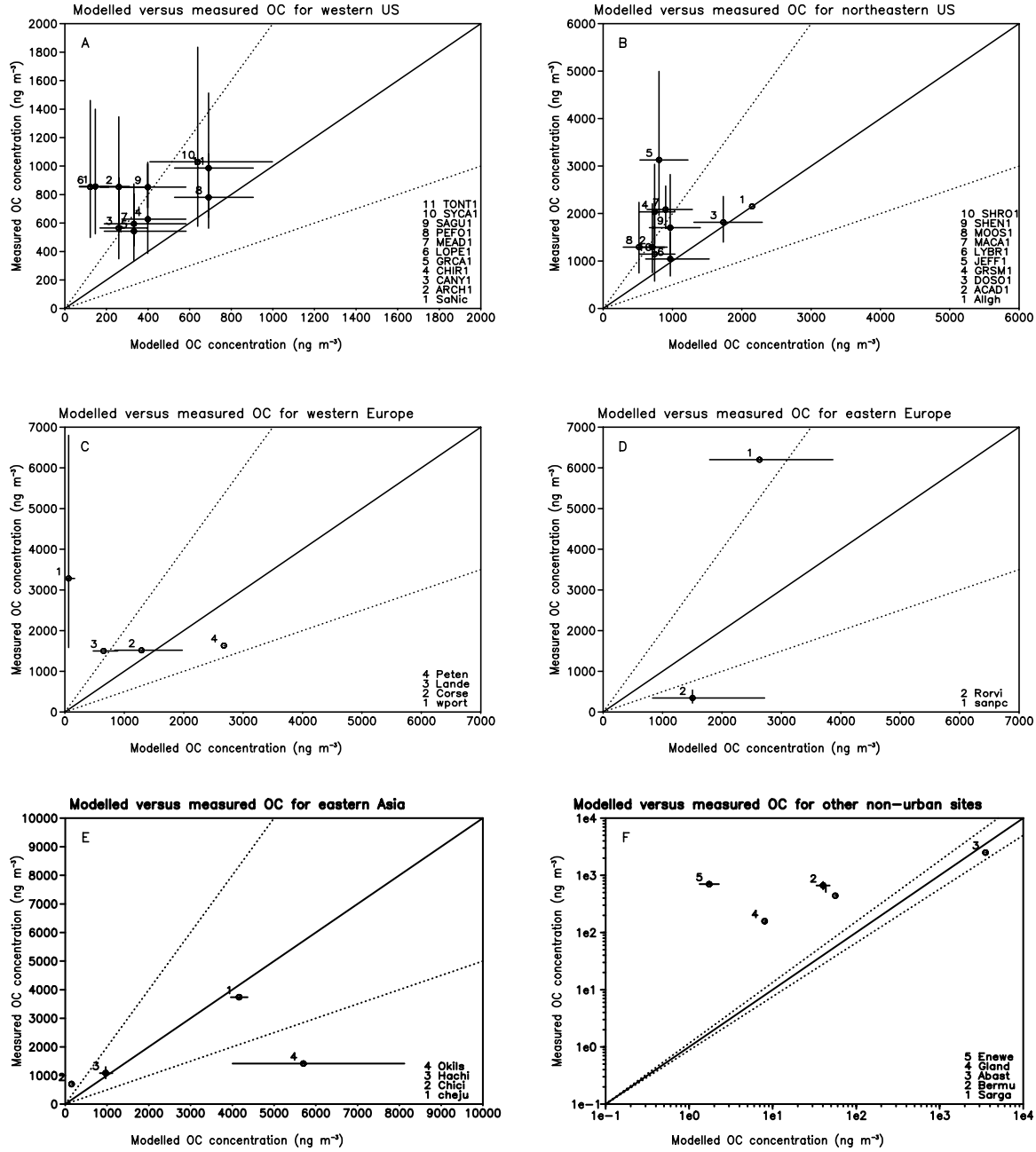


**Figure 12.** Comparison of modeled and measured OC at various sites. Horizontal and vertical bars denote the variability in the modeled and available measured concentrations, respectively. Dotted lines indicate a range of a factor of 2. Acronyms for the sites are explained in Appendix B. A 1 *Hidy et al.* [1974], 2–11 *Malm et al.* [1994], B 1 *Keeler et al.* [1990], 2–10 *Malm et al.* [1994], C 1 *Castro et al.* [1999], 2–3 *Cachier et al.* [1989b], 4 *Berner et al.* [1996] D 1 *Zappoli et al.* [1999], 2 *Brorström-Lundén et al.* [1994], E 1 *Kim et al.* [1999], 2–3 *Ohta and Okita* [1984], 4 *Mukai et al.* [1990], F 1 *Andreae et al.* [1984], 2 *Wolff et al.* [1986], 3 *Hoffman and Duce* [1977], 4 *Pertuisot* [1997], 5 *Cachier et al.* [1990].

[51] The simulated tracer concentration in air has been examined to some extent in sections 3.2 and 3.3. The vertical distribution of the formation of precipitation affects the deposition of the aerosol in that if the formation occurs in areas of the vertical column where the aerosol concentration is low, then the removal mechanism will underestimate the deposition. Whether this is a problem of the scheme that produces the precipitation or a problem with the aerosol transport is beyond the scope of this work.

[52] The frequency and intensity of the precipitation combine to give the total precipitation, which, in many models, compares well with monthly mean observations. However, the monthly mean model precipitation could be a combination of a high frequency of events combined with a low intensity per event of precipitation, a low frequency of events combined with a high intensity, or a combination in between that fortuitously results in a monthly mean precipitation that is close to the observed quantity. If the aerosol concentration

**Table 3.** Comparison of Modeled and Measured Wet Deposition of Particulate Organic Carbon in SKYHI[a]

| Station Name | Latitude | Longitude | Time Period | Wet Deposition, μg $L^{-1}$ | |
|---|---|---|---|---|---|
| | | | | Modeled | Measured |
| Rörvik | 57°12′N | 12°18′E | Dec–March | 45–526 | 237[b] |
| Mace Head | 53°18′N | 9°54′W | Oct–Nov 1989 | 12–52 | 69[c] |
| Porspoder | 48°30′N | 4°46′W | March 1994 | 128 | 135[d] |
| Gif-sur-Yvette | 48°N | 2°E | 1988–1990 | 365 | 851[c] |

[a]Range in the modeled values is the range of the monthly modeled means for the same period as the measurements.
[b]*Brorström-Lundén and Lovblad* [1991].
[c]*Ducret and Cachier* [1992].
[d]*Pertuisot* [1997].

in air were constant, this would not be a problem, as the removal process is modeled in a linear manner. However, the aerosol concentration does vary, and this will most likely lead to underestimates of the wet deposition flux for the following reason: A high-intensity rain event combined with a high aerosol concentration will result in a large flux to the surface. If the frequency of these types of events is deficient in the model, then the aerosol flux to the surface may be underestimated. In the case of high-frequency, low-intensity precipitation the flux of aerosol to the surface may be underestimated due to the underestimation of the deposition during high aerosol concentration periods.

[53] In this section the modeled precipitation is compared with the precipitation from the Global Precipitation Climatology Project (GPCP). The GPCP is an international effort organized by the Global Energy and Water Experiment/GEWEX Radiation Panel to provide an improved long-term precipitation record over the globe. The 36 monthly means of SKYHI precipitation are compared with 108 months (1988–1996) of the GPCP data set. It should be noted that the GPCP data extend from ~70°N to 50°S only. The monthly means of the observed and modeled precipitation are subjected to a t test to gauge the significance of differences in the means of the observed and modeled precipitation fields. The ratio of the means is shown in Figure 13, where the differences at the 99% significance level are shown. Most regions have insignificant differences. There are, however, several areas where the modeled means are significantly different, notably in regions

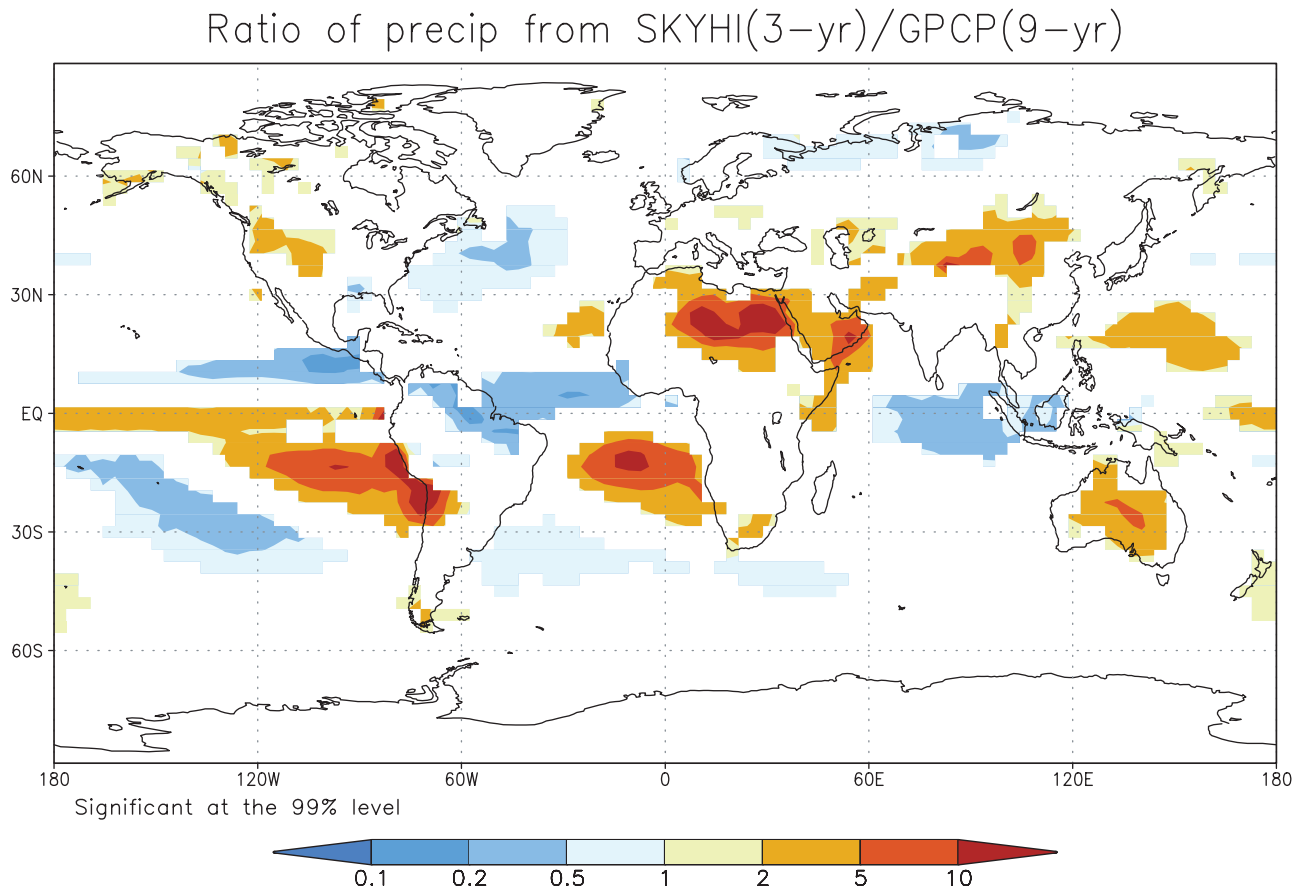


**Figure 13.** Ratio of annual mean precipitation from SKYHI model (3-year integration) and the Global Precipitation Climatology Project (1988–1996). Only regions with differences at the 99% significance level are shown.

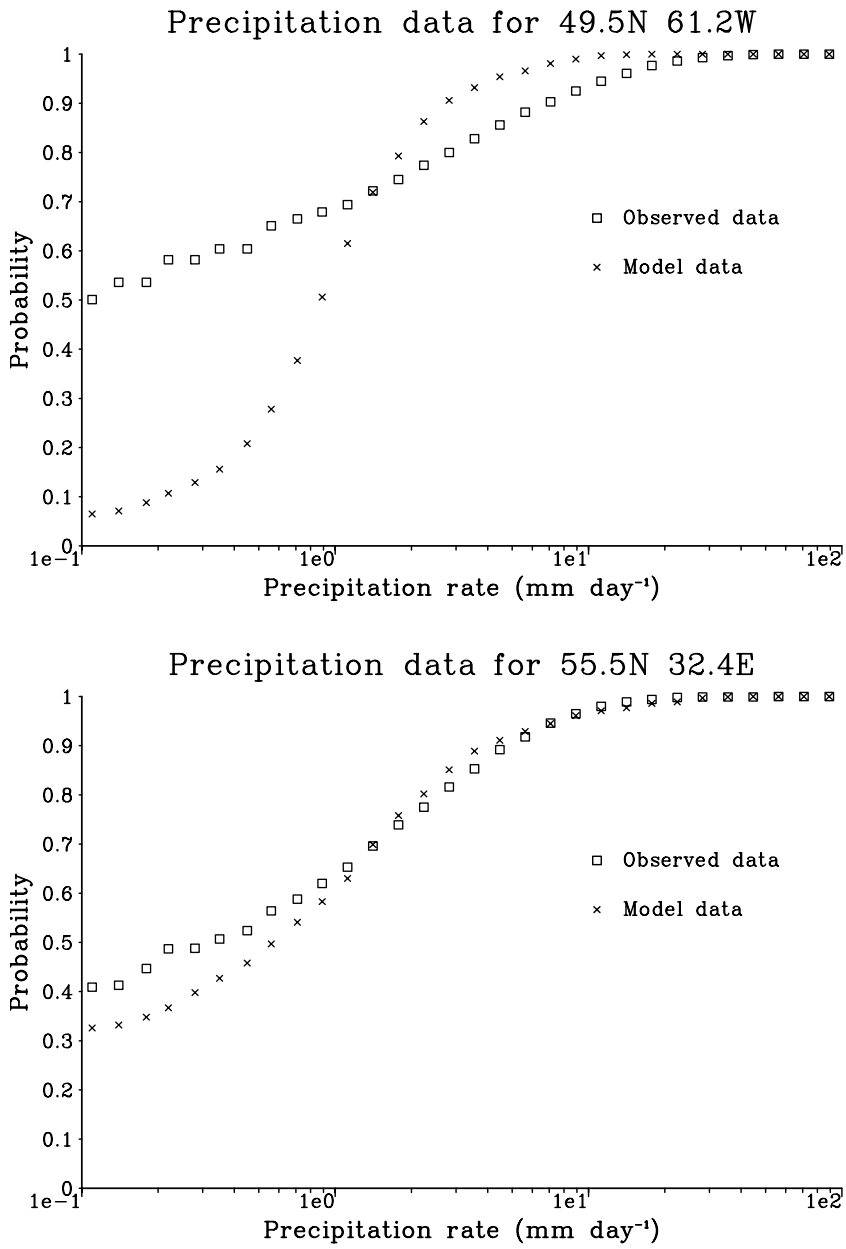


**Figure 14.** Cumulative probability of a daily mean precipitation rate being less than a specified rate for two grid boxes at two different geographical locations.

of stratus decks in the Southern Hemisphere. The difference in the area over the Sahara desert is probably not relevant, as the precipitation there is <0.05 mm day$^{-1}$ in the observations, so small changes at this level will produce what appear to be significant changes. The band of overestimation and underestimation in modeled precipitation in the Pacific between 180° and the Central American coast is due to a southerly bias of the precipitation maximum in the model in this region. Similarly, the overprediction in central Asia and the underprediction in the Indian Ocean are due to a northeasterly bias of the precipitation maximum in the Bay of Bengal.

[54] While the overall monthly mean precipitation is reasonably well modeled, one also needs to look at the distribution of precipitation at a higher frequency than the monthly level. To this end, observations of daily precipitation from 861 sites in the United States and Europe over periods of up to 25 years were obtained from the Utah Climate Center, which archives daily meteorological data in cooperation with the National Climatic Data Center (J. Lanzante, personal communication, 1999). Data from the available 861 sites were aggregated such that the observations from several sites contributed to the calculation of the mean precipitation within a grid box. If observations from more than one site within a grid box occurred on the same day, the arithmetic mean of the observations constituted the grid-box average for that day.

[55] The data thus organized were then used to compare the probability of occurrence of daily precipitation rates for the same grid box in the model and observation. Figure 14 compares the modeled and observed cumulative probability

of precipitation at less than a certain rate for two grid boxes at different locations. The lower limit of 0.1 mm day$^{-1}$ in Figure 14 is due to this being a lower limit of the rainfall rate at which wet deposition is allowed in the aerosol model and is also the lower limit in the observations. The offset from a probability of zero at precipitation rates of 0.1 mm day$^{-1}$ can be interpreted approximately as the fraction of days without precipitation. In Figure 14a (49.5°N, 61.2°W), ~50% of the days are dry in the observed data, while in the model this is <10%. It should be noted here that this grid box is ~6° north of Sable Island. Figure 14a also shows that the model tends to have a large number of days (~50%) when the precipitation rate is quite low (0.1 mm day$^{-1}$ < $P$ < 1 mm day$^{-1}$), while only 20% of observed precipitation events fall in this range. The fraction of precipitation events between 1 and 10 mm day$^{-1}$ is similar (roughly 30%) but is dominated by less intense events in this range in the case of the modeled precipitation. The annual mean precipitation in this grid box is 2.43 mm day$^{-1}$ in the observed data and is 1.52 mm day$^{-1}$ in the model.

[56] In some other grid boxes the agreement between the model and the observed data is much better, as in Figure 14b. This grid box is in contrast to that discussed above. Both the observed and modeled data have dry days for ~35% of the total period analyzed, and the data sets track each other well for increasing precipitation rates. In this case the observed and modeled annual mean precipitation rate were 1.84 and 1.96 mm day$^{-1}$, respectively. For the data examined here, one can say that one in eight of the grid boxes is in good agreement (compare Figure 14b), while the rest are between Figures 14a and 14b, with several being closer to Figure 14a. About 25% of the grid boxes in Europe are similar to Figure 14b, but only 2 of 95 grid boxes in the United States are in very good agreement. The disagreement in the United States arises from a region between 75°E and 90°E where the model predicts that most precipitation events occur at a rate of 1 mm day$^{-1}$ or less. Also, over the Rockies the model typically predicts that dry days occur 20% of the time, while 60–90% of the observations show dry days. In general, the best agreement of the distribution of precipitation intensity events is in continental regions, while there is an overprediction of low precipitation rates in marine situations.

## 4. Sensitivity Studies

[57] The previous results reveal that the model simulation does not exactly reproduce the available observations in all respects. This may be due to many factors. The aerosol model may be incorrect in the way it treats the transformation and deposition of the aerosol. The transport model may be deficient in certain areas of the globe. In order to get some insight into these deficiencies, we carry out sensitivity studies on various aspects of the model's simulation. In particular, we look at the sensitivity of the global distribution of carbonaceous aerosol due to variation of the various pathways (see Figure 1). There is no radiative feedback on the climate system from the carbonaceous aerosol in this study, so there will be no changes in the thermodynamics and transport features of the model due to the changes in the aerosol distribution. The analysis is performed by considering the concentration fields as simulated for the third year in the model run. We consider only the BC aerosol distribution.

[58] Before we investigate the sensitivity of the atmospheric aerosol to the model used, the results of the standard case are inspected. Figure 15a shows the annual mean column burden of BC. The column burden is one factor governing the distribution of the radiative effect of the aerosol. The height distribution is another important factor. The column burden in the atmosphere is a maximum over the source regions but is also important (>1% of the peak values) in remote regions. The peak of the distribution is over China and eastern Europe, where the emissions are the largest. There are also significant burdens over the eastern United States, western Russia, and India. One can notice that practically the entire Northern Hemisphere landmass is significantly affected by the aerosol, with nonnegligible burdens extending into the oceanic areas. The spread in the South Atlantic from the source regions in southern Africa and South America is also evident. The column burden is dominated by the aerosol concentration near the surface. In all but two of the sensitivity tests discussed in sections 4.1–4.5, the contribution of the layer from the surface to 700 hPa is between 66 and 73% of the total annual average column burden. The atmospheric layer between 400 and 700 hPa typically contributes 13–17%, while the layer between 100 and 400 hPa contributes 9–14%. Above 100 hPa the contribution is typically 3%.

[59] Figure 15b shows the annual zonal mean BC concentration. For a given altitude the greatest concentrations are, not surprisingly, confined to the latitudes where the emissions of BC are greatest, namely, midlatitude Northern Hemisphere. However, a relatively significant amount of BC is advected to the upper troposphere (>1 ng m$^{-3}$). As shown in Figure 10, the model appears to overestimate the BC concentrations in this region of the atmosphere, although it should be remembered that there are large uncertainties in the measurements due to the difficulties of sampling at these heights. In addition, the model run of 3 years is probably too short to allow equilibrium to be reached for aerosol in the stratosphere. It would appear that BC is being lofted to the upper troposphere where there are no chemical sinks, and some other sink has to be included in the aerosol model in order to prevent the model from accumulating BC aerosol in the upper atmosphere. It should be noted here that in the Antarctic the column burden appears to be dominated by concentrations in the 200- to 300-hPa range, and the sensitivity in this region to changes in parameters will accordingly be controlled by changes in concentrations at this level.

[60] Figure 1 shows that there are five potential governing parameters, namely, (1) the total aerosol emission, (2) the fraction of aerosol emitted as hydrophobic and hydrophilic aerosol, (3) the transformation time, (4) the dry deposition, and (5) the wet deposition rate of the aerosol. In each of the sensitivity tests discussed in sections 4.1–4.5, the standard model parameters were used as a basis, with the parameter of interest being the only one to change. The annual average global burdens and the variations thereof due to the sensitivity studies are given in Table 4.

[61] In Figures 16–20 the ratios of the column burdens and zonal mean concentrations for the third model year are shown. The 365 daily values in each run are used to

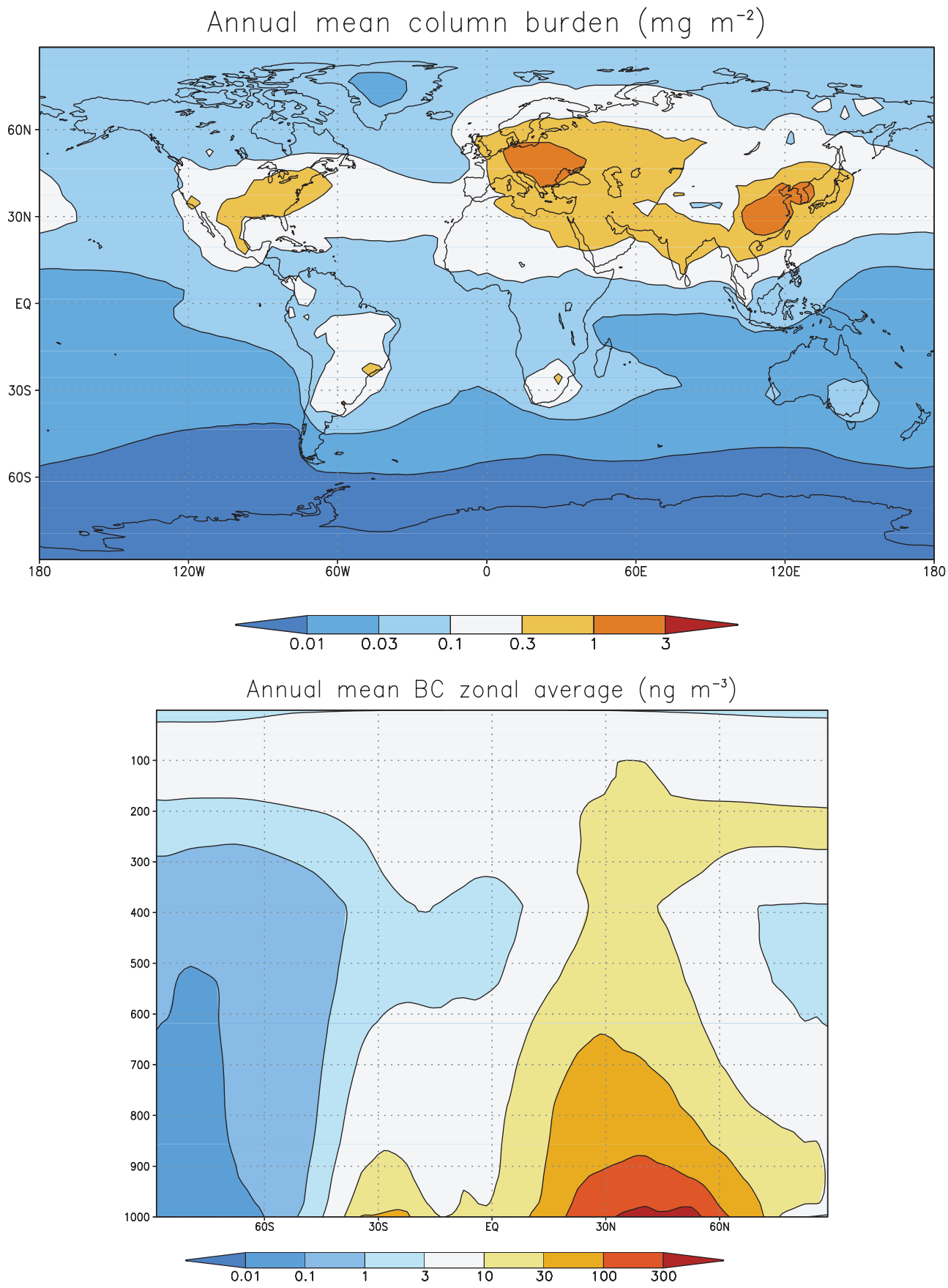


**Figure 15.** Simulated (a) annual mean and (b) zonal annual mean of column burden distribution of BC in milligrams per square meter. This is referred to as the "standard" distribution.

**Table 4.** Sensitivity of Global Mean Atmospheric Burden and Lifetime of BC Aerosol to Variations in Different Parameters

| Parameter | Burden, Tg | Lifetime, days |
|---|---|---|
| Standard | 0.060 | 4.29 |
| Transformation time halved | 0.045 | 3.22 |
| Transformation time doubled | 0.064 | 4.58 |
| 90% hydrophobic emission | 0.066 | 4.72 |
| 100% hydrophobic emission | 0.069 | 4.94 |
| 100% soluble aerosol | 0.033 | 2.36 |
| Wet deposition rate halved | 0.079 | 5.65 |
| No wet deposition allowed | 1.593 | 114.0 |

calculate the mean and standard deviation, and a students t test is performed to see if changes due to the sensitivity test are significant. The ratios are only shown where the change is statistically significant at the 99% level. The lack of significance simply implies that the model variability dominates over the magnitude of the change brought about due to a change in the parameter concerned.

### 4.1. Sensitivity to Transformation Timescale Parameterization

[62] The timescale ($\lambda$ in Figure 1) of the transformation of hydrophobic to hydrophilic carbonaceous aerosol is not known with any great certainty. Previous studies [*Cooke and Wilson*, 1996; *Cooke et al.*, 1999] have assumed, for simplicity, a timescale of $\sim$1 day. A sensitivity test for this parameterization is performed by doubling and halving the time needed to transform the hydrophobic aerosol into hydrophilic aerosol. When the timescale is halved, the hydrophobic aerosol transforms to hydrophilic aerosol more quickly and is thus rapidly available for wet deposition. The aerosol distribution is therefore more conducive to being removed, and the aerosol burden is lowered. One can see from Table 4 that on a global scale, halving the transformation time of the hydrophobic aerosol decreases the atmospheric burden by 25% and doubling the transformation time increases the burden by 7%.

[63] The effect of varying the timescale is shown in Figures 16 and 17, where the timescale has been changed from its standard value of 1 day by a factor of 0.5 and 2, respectively. From Figure 16a, halving the transformation time produces more hydrophilic aerosol early enough, and this decreases the annual average column burden by at least 10% in all areas of the globe. Over the Northern Hemisphere oceans the reduction can be up to 60%. Near the major source regions of the northeast United States, Europe, and China the reductions are still at least 20%, which may appear a little surprising as one might expect that the aged aerosol would not be scavenged so quickly. However, the short lifetime of the hydrophobic aerosol means that the aerosol will not be transported over very large distances before it is removed by wet deposition processes. Over Antarctica the fractional reduction is less, although the column burden in this region is quite low in the standard case. This diminution in the relative decrease of the column burden shows that hydrophobic aerosol persists in the atmosphere over the entire globe.

[64] In the zonal mean profile shown in Figure 16b, there are statistically significant changes throughout the troposphere, with reductions of at least 20% in the entire lower troposphere. This can be attributed to the more hydrophilic nature of the aerosol, which can therefore interact with the precipitation and be removed.

[65] The effect of doubling the time needed to transform the hydrophobic aerosol to hydrophilic aerosol should result in a less hydrophilic aerosol and therefore in greater burdens. From Table 4 and Figure 17a it is evident that this holds true. In remote regions the effect is to increase the burdens by >50%, and in less remote regions the effect is to increase the burden by at least 20%. Over the Arctic region the column burden is greatly increased. The radiative implication of this effect is negligible at this time of year but could be important with the onset of spring. When compared to the case where the transformation time is halved, there are large areas of the globe where there are no statistically significant changes in the column burden.

[66] In the zonal mean distribution shown in Figure 17b, there are also significant increases in the concentrations, particularly around the 500-hPa level. Consistent with Figure 17a, there is generally little statistical significance in the lower troposphere in low and middle latitudes. In the troposphere the magnitudes of the relative increases mirror that of the decreases found when the transformation time was halved. In the Arctic region the column burden increase is mainly due to the increase in concentration in the middle troposphere (500–700 hPa). Figures 16 and 17 point to the very large effect of the transformation time parameter in governing both the column burden and the height distribution.

### 4.2. Sensitivity to Emission Partition Parameterization

[67] The standard model assumes that 80% of the BC emissions are hydrophobic and 20% are hydrophilic. BC is thought to be hydrophobic when freshly emitted but is incorporated into rainfall near to source regions, which implies that a fraction of the aerosol is hydrophilic to some extent. The sensitivity of the aerosol burden to the emission partition can be tested by assuming that 90 and 100%, in respective tests, of the aerosol is emitted in the hydrophobic form. Therefore it can be expected that the aerosol will be more hydrophobic and will result in an increased burden. From Table 4, the global annual average burden increases by 10 and 15%, in respective tests, relative to the standard case. Figure 18a shows the annual average regional variation of this ratio when the emissions are 100% hydrophobic. In the case of 100% hydrophobic emission the differences are significant only in certain areas of the globe. This can be attributed to the overall increase in the atmospheric burden of 15%, which leads to overall higher concentrations. Note that this change is less than in the sensitivity tests for changes in the transformation time. The main areas where significant changes occur are in the central ocean regions. In the central Pacific, south of the equator, there is a region of increased column burden similar to the increase seen in the case of doubling the transformation time, and this may also be attributed to the greater hydrophobicity of the initial aerosol.

[68] For the case where 90% of the emissions are hydrophobic (not shown here) the changes in the column burden are statistically insignificant over large regions of the globe. The positioning of the areas of significant differences is similar to the 100% hydrophobic emission case but, generally, these areas have a lesser areal extent.

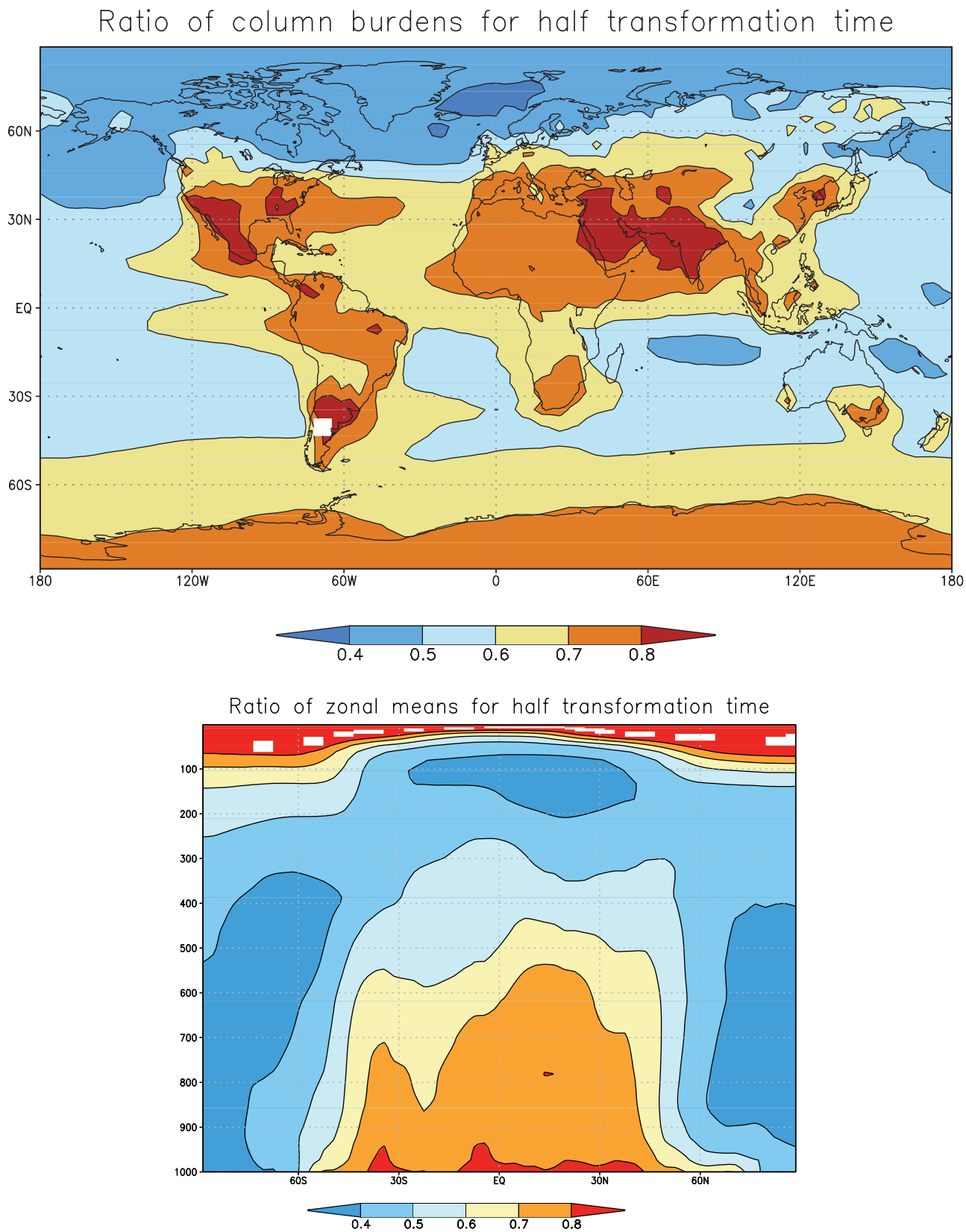


**Figure 16.** Ratio of (a) column burden and (b) zonal mean concentration of BC compared to standard distribution when the transformation time is halved. White denotes areas where the changes are not significant at the 99% confidence level.

[69] The vertical distribution of BC due to change in the emission partition is shown in Figure 18b. The changes in the concentrations are reasonably similar for both the 90 and 100% cases. The significant changes in the aerosol concentration are confined mainly to the polar regions and to the upper troposphere. The most significant detail is the large ratio increase over the Antarctic region. Because of the high surface albedo here, the radiative implication of this effect could be quite important.

[70] As the comparisons of the wet deposition of BC and OC and the vertical distribution of BC have shown, there may be some weaknesses in the scavenging scheme in this model. A lower limit can be put on the burden of aerosol by allowing the emitted aerosol to be completely soluble. In this case the aerosol would be removed more rapidly, and this should lead to an aerosol with the shortest possible lifetime and lowest burden. As seen in Table 4, the global effect of having 100% hydrophilic emissions is to reduce the aerosol burden by 45%. On a regional basis, from Figure 19a, the column burden of aerosol is significantly reduced in most areas. Over the Arctic and northern mid-oceans the column burden is reduced by a factor of at least 3. Over the oceans the effect is to reduce the burden of aerosol by at least 60%. The smallest effect is over the Arabian sea and the southwest United States. These are desert regions where there is little removal by rain. In the zonal average (Figure 19b), there is also a general decrease in the zonal mean concentration, and the greatest effect is seen over the Arctic region. Concentrations in the upper troposphere are also reduced by a factor of 3. In this case the lower troposphere contributes 78% of the aerosol burden. Thus the physical characteristics of the aerosol discussed in sections 4.1 and 4.2 can yield a range of a factor of 2 in the global burden and lifetime. This uncertainty is in addition to the biases that may arise due to the model's transport and scavenging simulation processes.

### 4.3. Sensitivity to Total Emission

[71] The emissions of *Cooke et al.* [1999] are thought to be uncertain to at least a factor of 2. The atmospheric burden of aerosol is linear with emission strength. Therefore no results for variation of aerosol source strength are shown. However, one can simply scale the results given here to obtain the burdens for other source strengths.

### 4.4. Sensitivity to Dry Deposition Parameterization

[72] The dry deposition of aerosol is a minor, although nonnegligible, sink for aerosol. In this model the annual average dry deposition accounts for ~5% of the flux to the surface. Dry deposition only occurs at the surface, however, and it will not severely affect the column burden of aerosol. For this reason we do not show any results for variation of the dry deposition parameterization.

### 4.5. Sensitivity to Wet Deposition Parameterization

[73] The effect of the wet deposition scheme can be approximately examined by halving and removing the wet deposition of hydrophilic aerosol. From Table 4, the annual burden is increased by 30% when the deposition is halved and is increased by a factor of 25 when the wet deposition is switched off entirely, a hypothetical case considered for comparison purposes only. Figure 20a shows the ratio of the burdens when the wet deposition is halved. The burden increases by at least 40% over almost all of the oceanic areas. The greatest effect can be seen over the Arctic region, with a doubling of the column burden over a significant fraction of the area. This is due to the overall diminution of the scavenging of the aerosol, resulting in a greater fraction of aerosol being transported to these remote regions. In the area east of Papua New Guinea the increase in column burden can be attributed to the decrease in scavenging by the intense precipitation in this region. For the case when the wet deposition is switched off entirely, the regional effect is much higher (results not shown here), with ratios of at least 5 and, in some regions, greater than 100.

[74] In Figure 20b the effect of halving the wet deposition has the greatest effect in the middle troposphere (300–700 hPa); the concentrations are also most sensitive close to the surface at high latitudes. In the Arctic the concentrations nearer the surface govern the overall column burden, with the sensitivity maximized in the zonal mean concentrations between 400 hPa and the surface being similar in magnitude to that in the column burden. In the Antarctic the column burden appears to be dominated by concentrations in the 100- to 200-hPa range, with the sensitivity in the zonal mean at 100–200 hPa being similar to that in the column burden for this region. Referring to the zonal mean of the standard model (Figure 15b), the zonal mean concentration is indeed greatest over Antarctica at the 100- to 200-hPa level. For the case when the wet deposition is switched off entirely, the atmospheric burden in the lower troposphere (surface to 700 hPa) contributes only 38% of the burden.

### 4.6. Variability of the Aerosol Concentration at the Surface From the Sensitivity Tests

[75] Figure 21 shows the 3-year mean and the maximum and minimum monthly mean values for each sensitivity test for each of the four long-term sites where a comparison was made earlier (section 3.2.1 and Figures 2, 3, 4, and 6). The annual mean and maximum and minimum monthly means are also given for the observations. The direction of the sensitivity for all but one (doubling of transformation time) of the parameters is the same at each of the four sites.

[76] In general, the range of the simulated aerosol concentrations in the monthly means is underestimated, with the best agreement being at Mauna Loa and Mace Head. At Mace Head the large variability in the modeled concentrations is mainly due to the variability of the concentrations during August and September (Figure 6). Looking at seasonal comparisons of the variability during periods other than August and September (not shown here), the modeled range is much closer to the observed range. The longer time period of measurements at Mauna Loa and Mace Head as compared to Sable Island and Bondville may also account for some of the discrepancies at the latter locations (compare section 3.2.1).

[77] The changes in the transformation time of the hydrophobic to hydrophilic aerosol in Figure 21 are discussed first. The case where the transformation time is doubled results in a 10% decrease in the mean concentration at Bondville but results in an increase in the concentration at the other three sites, as might be expected from a more hydrophobic aerosol. As Bondville is the most anthropogenically influenced of the sites, it is probable that this is

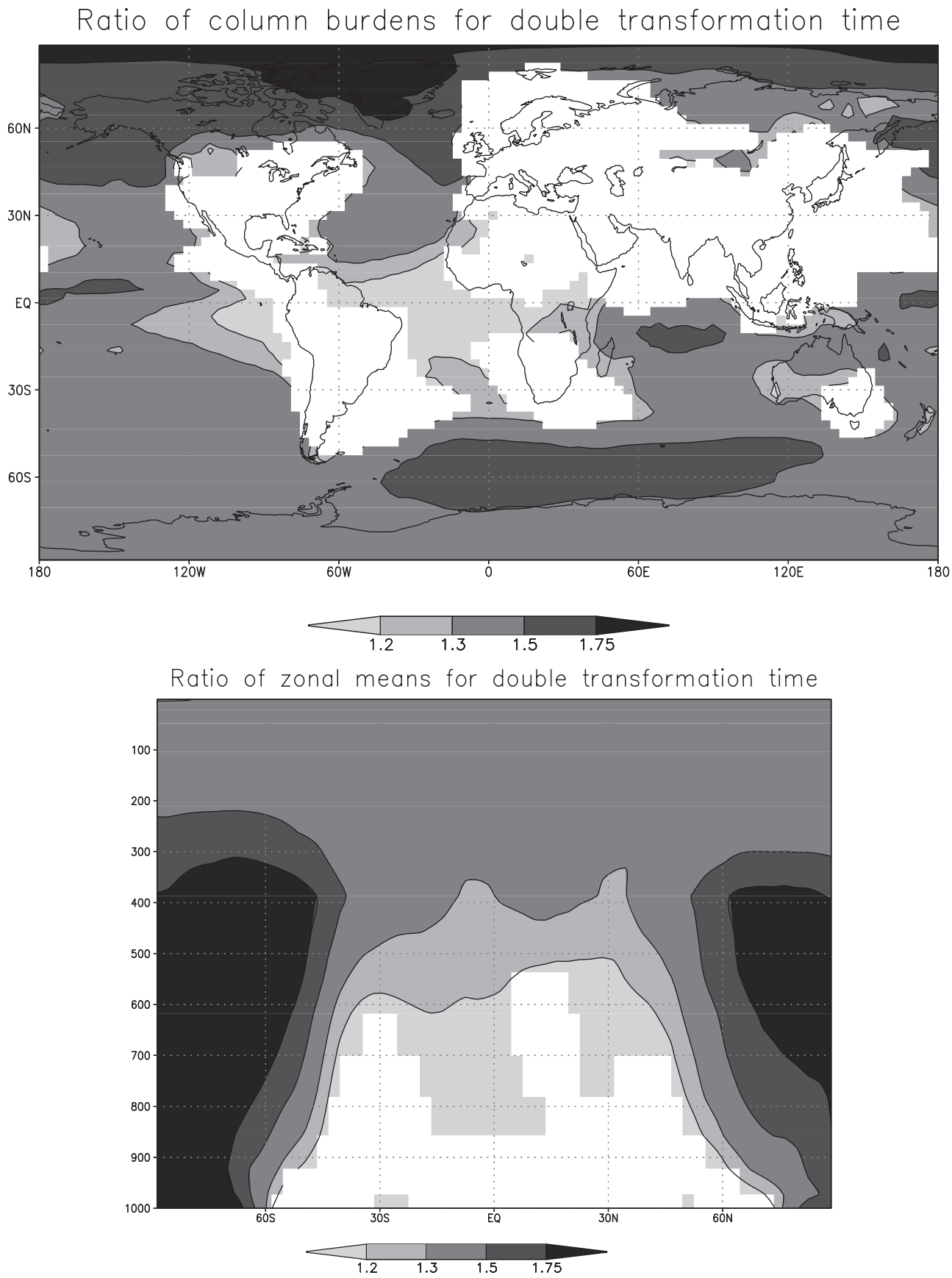


**Figure 17.** Ratio of (a) column burden and (b) zonal mean concentration of BC compared to standard distribution when the transformation time is doubled. White denotes areas where the changes are not significant at the 99% confidence level.

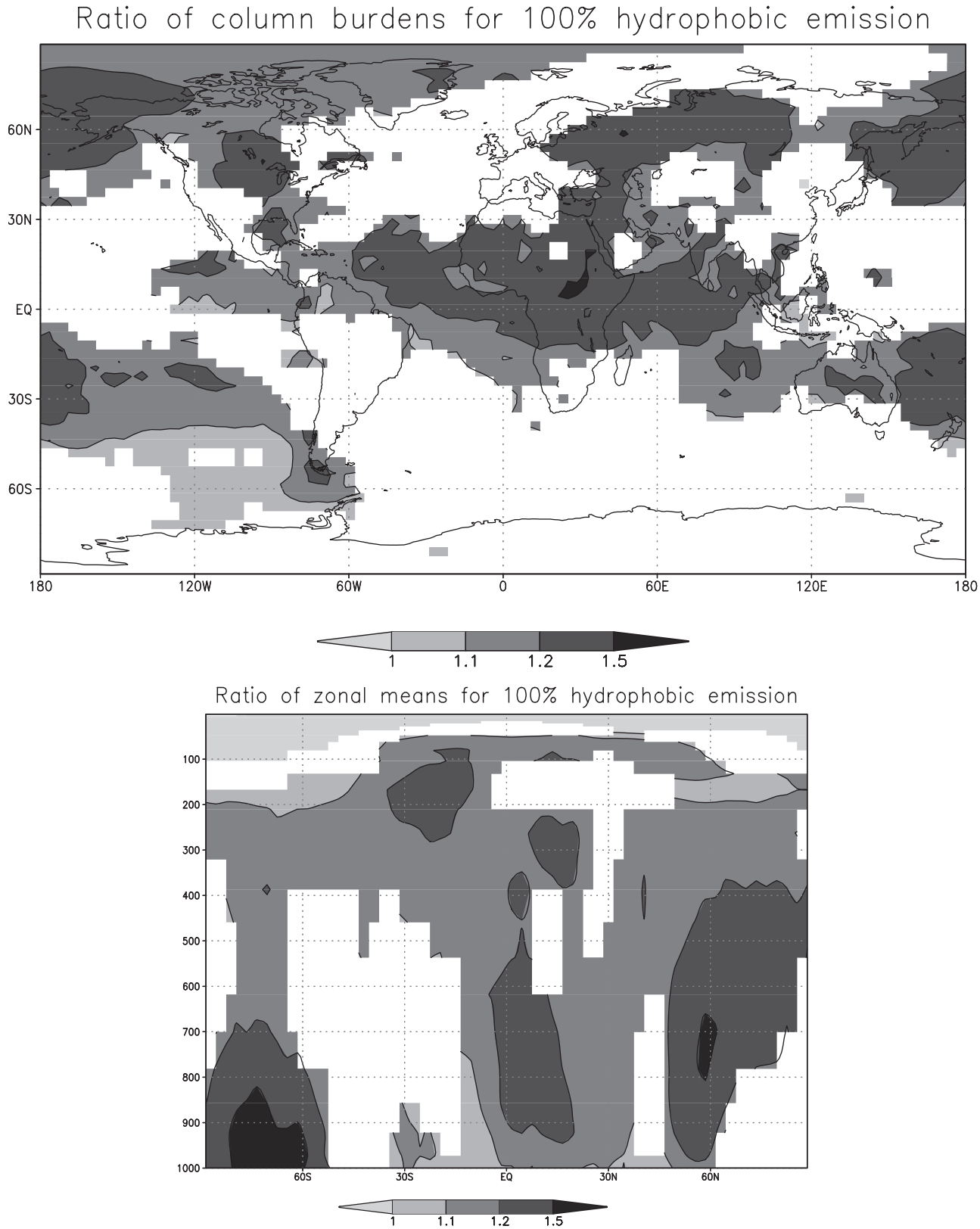


**Figure 18.** Ratio of (a) column burden and (b) zonal mean concentration of BC compared to standard distribution when the emissions are 100% hydrophobic. White denotes areas where the changes are not significant at the 99% confidence level.

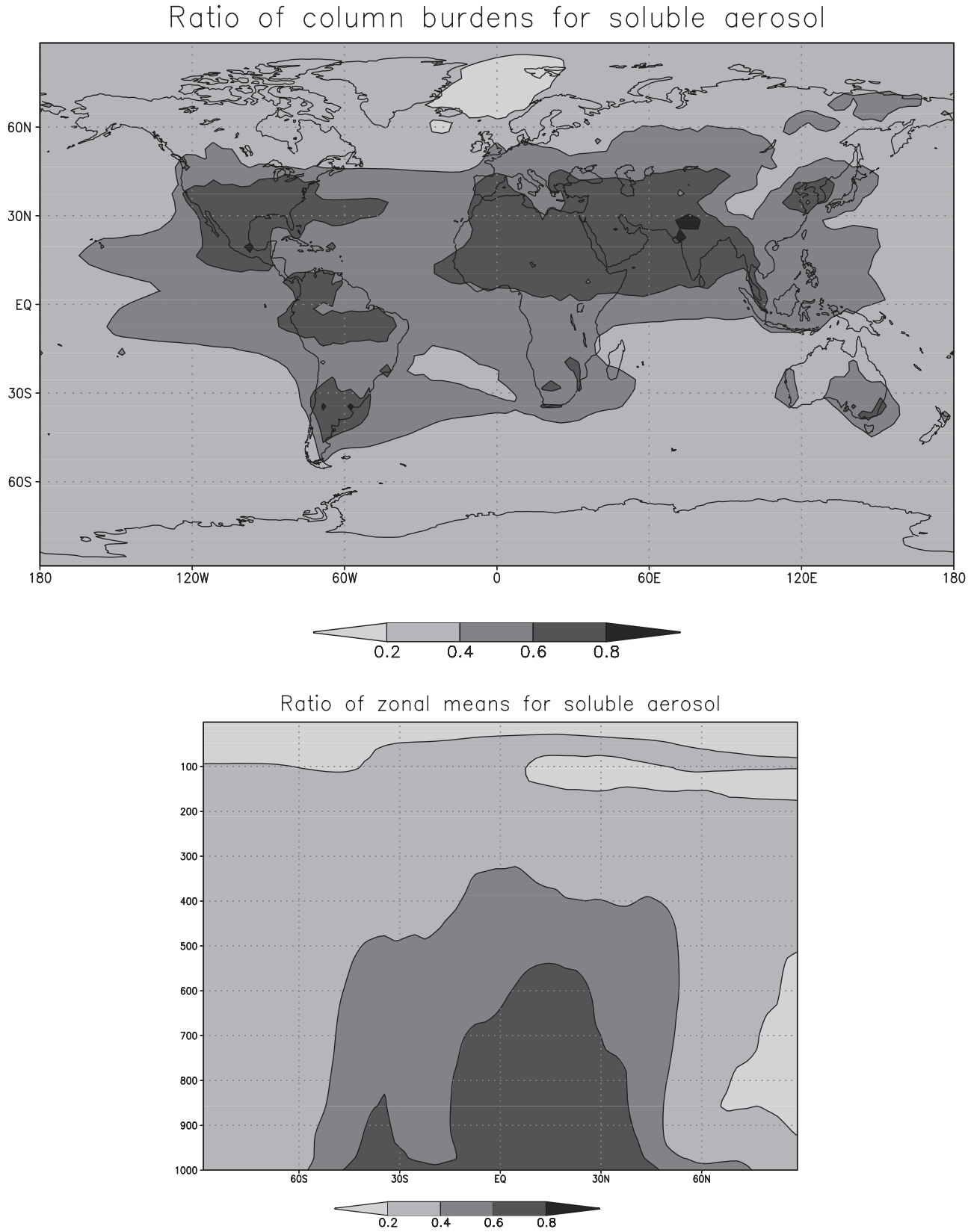


**Figure 19.** Ratio of (a) column burden and (b) zonal mean concentration of BC compared to standard distribution when the emissions are entirely hydrophilic.

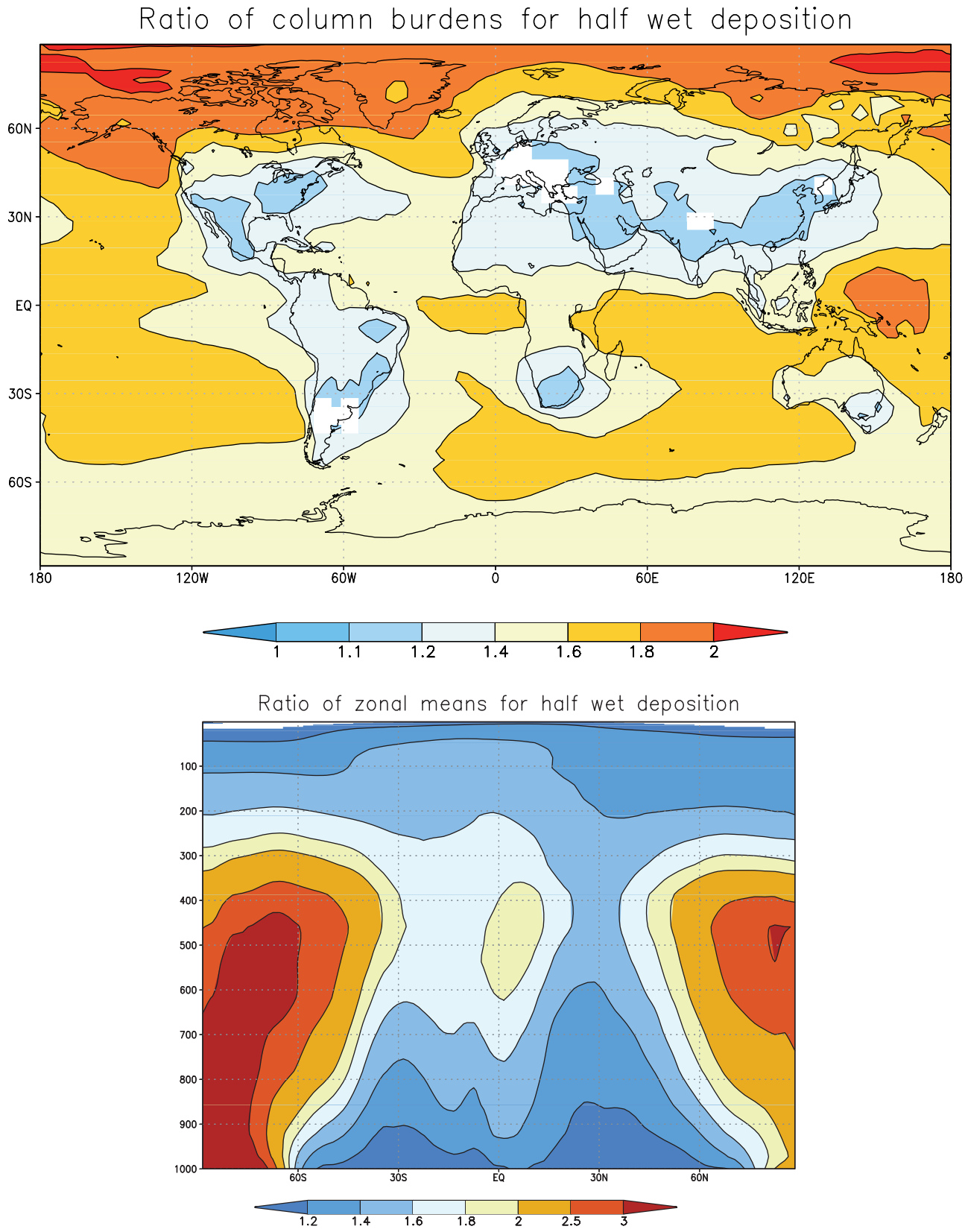


**Figure 20.** Ratio of (a) column burden and (b) zonal mean concentration of BC compared to standard distribution when the wet deposition is halved. White denotes areas where the changes are not significant at the 99% confidence level.

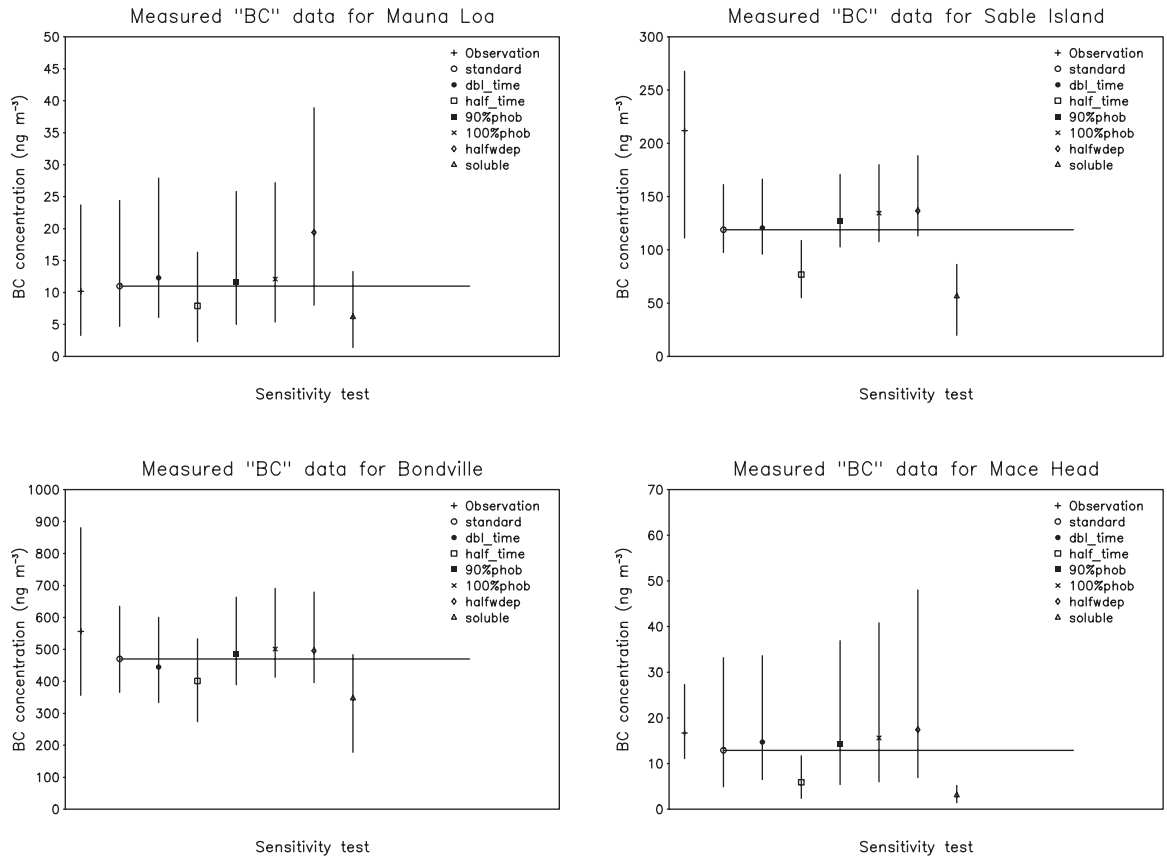


**Figure 21.** Sensitivity of modeled annual mean surface concentrations at the four long-term sites to the various sensitivity tests (see section 4). Maximum and minimum monthly values, which constitute the range in observations and in each of the sensitivity tests, are also depicted. For reference, a horizontal line is drawn at the 3-year mean for the standard run.

due to fluctuations in the large concentrations to be found near the emission sources of the eastern United States. In any case, the sensitivity of the global mean aerosol concentration to doubling the time of this parameter is not very large (Table 4).

[78] At each site, halving the transformation time, which leads to an increase in the hydrophilic aerosol content, reduces the mean atmospheric concentration. The range of the aerosol concentration is also decreased as the aerosol is removed more efficiently. At Mace Head the range of the aerosol concentrations is much less for this case and is even less than the observed range. This may be a coincidence as the variability at the other sites, in contrast, is relatively insensitive to the various parameters. The Mace Head results would suggest that the lifetime of the hydrophobic aerosol prescribed in models should probably be reduced, as it is important to correctly simulate the variability of the aerosol concentration. However, several short-term measurement sites in the Arctic are in better agreement when the transformation time is doubled (not shown). Thus, examining results for one location is not adequate to ascertain the causes of the biases.

[79] The hydrophobicity of the initial emissions does not appear to have a large effect on the annual mean or range in the monthly means at any site. The lack of sensitivity at the remote sites to the hydrophobic nature of the initial emissions shows that the concentrations are dominated by the effects due to transport and wet deposition on the hydrophilic fraction of the aerosol. At Bondville, there is some sensitivity to the hydrophobic nature of the emissions, with increasing phobicity leading to slightly increased concentrations. However, the relative increase in concentrations, considering all sites, is changed by <10%.

[80] The wet deposition rate of the aerosol has a relatively greater impact on the overall mean surface concentration at the four sites. Close to (Bondville) and downwind of (Sable Island) sources the sensitivity of the mean concentration to the wet deposition rate of aerosol appears to be relatively weak. At Bondville and Sable Island the mean concentration increases by <10%. This implies that the rate of wet deposition is apparently less influential in affecting the concentrations at these sites in the model. At Bondville this is to be expected, as the aerosol concentration is dominated by the initial emissions, and wet deposition is not expected to have a substantially large effect on the concentrations. At Sable Island one might expect a greater sensitivity to the wet deposition parameter, as the transport time from the emission region of the northeastern United States is several days. However, if the frequency of removal by precipitation is high (section 3.4), then the overall removal will be insensitive to the absolute value of the removal parameter. As shown in Figure 14a, the precipitation frequency near

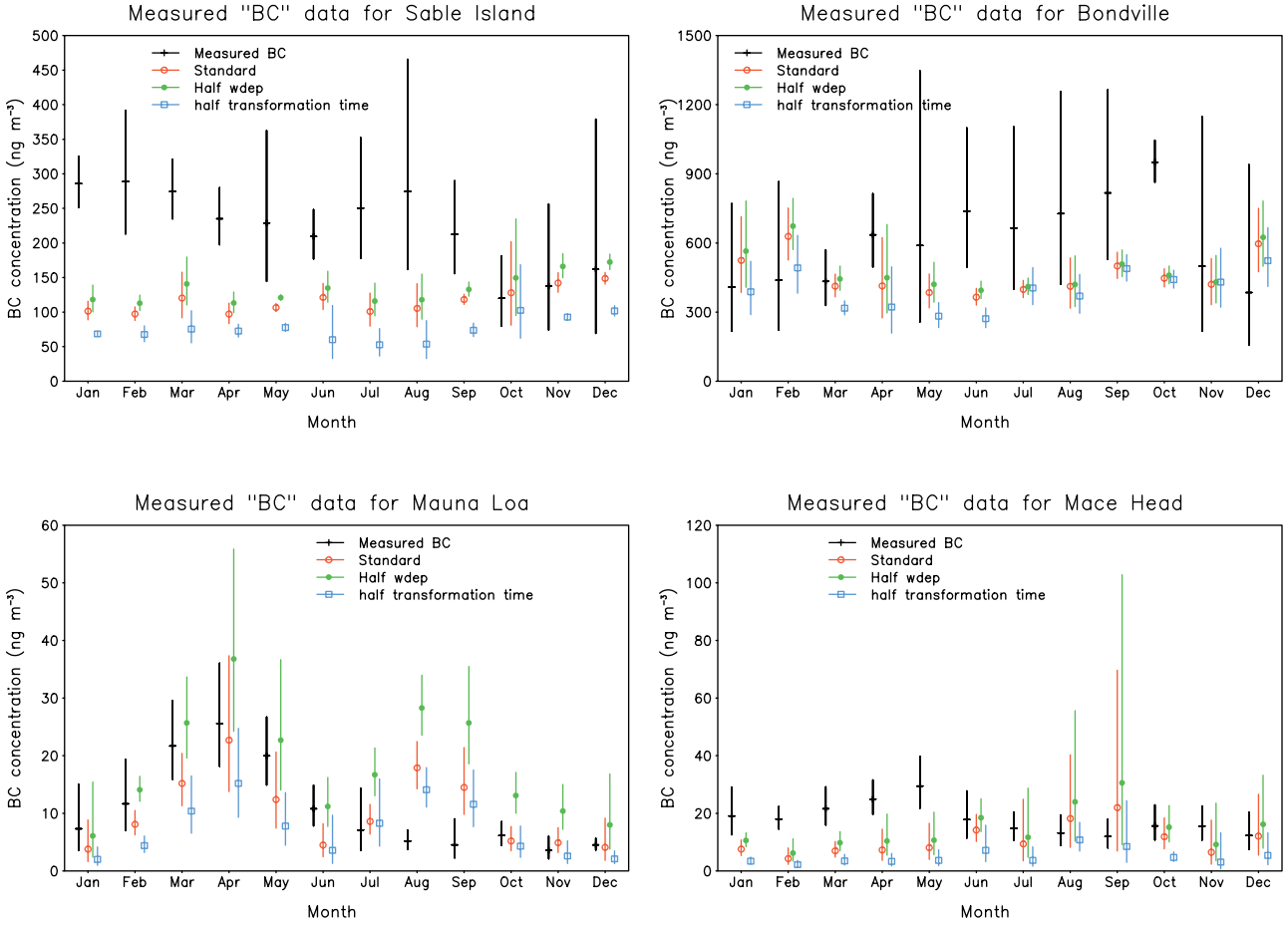


**Figure 22.** Sensitivity of modeled monthly mean surface concentrations at the four long-term sites to variation of the wet deposition and transformation timescales. Maximum and minimum monthly values, which constitute the range in observations and in each of the sensitivity tests, are also depicted.

Sable Island is overestimated. Therefore, in this region a small fraction is removed over a large number of time steps, and a saturation effect occurs whereby the removal is maximized regardless of the removal rate by wet deposition. If the removal frequency is reduced, it is likely that the overall concentrations would increase substantially for all the cases shown here, bringing the mean concentration closer to the observed value. At the more remote sites of Mace Head and Mauna Loa the wet deposition rate has a much greater effect on the mean concentration and the range, emphasizing the relatively greater effect of the wet deposition rate on long-range transport of the aerosol.

[81] Finally, the sensitivity to having completely soluble initial emissions is discussed. In all cases the aerosol concentration is reduced substantially, with the greatest effect being seen at Sable Island and Mace Head. The large decrease in the aerosol concentration at Sable Island reinforces the idea that the removal of aerosol is maximized during transport from the source in this region. At Mace Head the modeled and measured concentrations are from the marine sector, so the transport time is probably >5 days, on average. This allows for more interaction with precipitation events and for a reduction in the aerosol concentration. At Mauna Loa the reduction in sensitivity to soluble emissions may be due to the height of the station and the transport of aerosol above the clouds to this site. From studying the sensitivity of the aerosol concentrations at these sites to the various parameters, it is clear that uncertainties in aerosol physical characteristics, and modeled frequency and intensity of precipitation, play critical roles in model-observation comparison.

[82] In Figure 22 the monthly variations due to halving the wet deposition rate and transformation time for hydrophobic to hydrophilic aerosol are examined. These tests were chosen as they constitute an envelope of the sensitivities discussed above. In contrast to Figures 2–6, the geometric mean and deviation of the model results are shown here. From the sensitivity of the global burden, one could expect an increase of 32% in the concentrations when the wet deposition rate is halved as compared to the standard case (Table 4). This is a global and annualized average value, however, with the greatest effect seen in more remote regions (compare Figure 20a). The least effect is seen at Bondville, where the maximum monthly increase due to this effect is 9.3% (May). At Sable Island, there is an 11–17% increase in the surface concentration of aerosol. The fact that this is half of the global average increase due to halving the wet deposition rate provides further evidence of a saturation effect in the removal of aerosol in this region of the globe; that is, the removal of aerosol is so quick that

**Table 5a.** Sensitivity of Modeled and Measured Wet Deposition of BC to Parameter Changes in SKYHI[a]

| Station Name | Modeled | | | Measured |
|---|---|---|---|---|
| | Standard | Halved Wet Deposition | Halved Transformation Time | |
| Alert | 1.7–3.5 | 0.9–1.8 | 0.8–1.8 | 45.5 (0–127)[b] |
| Greenland Sea | 4.3 | 2.2 | 2.3 | 38.7 (5.4–75.5)[b] |
| Spitzbergen | 5.3 | 2.9 | 3.0 | 31 (6.7–52)[b] |
| Summit | 4.8 | 2.5 | 2.5 | 5.4[c] |
| Barrow | 6.2–8.4 | 3.5–4.7 | 3.8–5.6 | 23 (7.3–60.4)[b] |
| Abisko | 35.9–94.5 | 20.8–53.5 | 30.1–67.8 | 33 (8.8–77)[b] |
| Northern Sweden | 17.2–94.5 | 10.3–53.5 | 13.0–67.8 | 172 (30–700)[d] |
| Southern Sweden | 47.8–115.1 | 30.4–71.1 | 46.4–103.8 | 193 (20–600)[d] |
| Mace Head | 5.3–16.7 | 2.8–9.0 | 3.3–13.0 | 31 (9–94)[e] |
| Gif sur Yvette | 125.0 | 77.3 | 141.5 | 333 (27–1348)[e] |
| Porspoder | 32.4 | 20.9 | 32.5 | 31[c] |
| Hurricane Hill | 12.7 | 7.0 | 10.5 | 14.7 (10.1–18.5)[b] |
| Seattle | 44.7–55.5 | 32.9–42.3 | 54.2–68.1 | 60 (28–130)[d] |
| Halifax | 34.1–52.9 | 19.2–35.2 | 34.5–58.5 | 2.6–6.3[f] |
| Bridgewater, Nova Scotia | 34.1–66.4 | 19.2–44.8 | 34.5–69.7 | 0.5–8.2[f] |

[a]Range in the modeled values is the range of the monthly modeled means for the same period as the measurements. All measurements are in micrograms per liter.
[b]*Clarke and Noone* [1985].
[c]*Pertuisot* [1997].
[d]*Ogren et al.* [1984].
[e]*Ducret and Cachier* [1992].
[f]*Chýlek et al.* [1999].

halving that rate has no effect. At Mace Head the effect of halving the wet deposition rate is to increase the surface concentration by 24–44%. In August (32% increase) and September (39% increase) the variability of the aerosol is increased substantially. At Mauna Loa the effect of halving the wet deposition rate is greatest, with increases in concentration of 58% (August) to 152% (October). In addition to the concentration, the variability is also increased.

[83] With regard to the variation of transformation time, one can expect a decrease of 25% in surface concentration (Table 4) when the time for transformation of hydrophobic to hydrophilic aerosol is halved. At Bondville the effect is less, as this is near a source region, so that the emissions control the concentration. At Sable Island the reduction is between 20 and 50%. In this case the agreement between the modeled and measured concentrations is less. Owing to the excess removal of aerosol in this region, as hypothesized above, this is not surprising. At Mace Head the surface concentrations are reduced by 40% (August) to 61% (September). While halving the transformation time does tend to underestimate the surface concentration, it also reduces the variability, especially in August and September. From the reduction in the variability at this site, it might be concluded that the reduction in time for transformation of the aerosol is necessary, as the variability in the measurements are then followed more closely. However, comparisons of modeled concentrations with measurements at remote Arctic sites show a degradation of agreement when the time is halved. In fact, when the timescale is doubled, there is a marked improvement in the agreement. At Mauna Loa the concentrations are reduced by 3.5% (July) to 49% (December).

[84] The model-simulated concentrations are sensitive to wet deposition, variation in transformation time, and partition of emitted aerosol. In addition, the transport of aerosols away from source regions is governed by meteorology. Thus any comparison with observations and the resulting inferences in general have to recognize the roles played by each one of the above factors and not just the effect due to a single factor alone. However, it is possible that for specific sites any one of the above factors could play a more dominant role than the others.

### 4.7. Variability of the Wet Deposition From the Sensitivity Tests

[85] The sensitivity of wet deposition concentrations to halving the wet deposition rate and transformation times is shown in Table 5a, while that of the flux is shown in Table 5b. It can be expected that halving the wet deposition rate will result in deposition concentrations that are half that of the standard case. While there is a substantial reduction in the concentration of aerosol in precipitation, it is reduced by <50%. This can be explained by the higher air concentrations as a result of the lower deposition, which causes more aerosols to be removed at every precipitation event,

**Table 5b.** Sensitivity of Modeled and Measured Wet Deposition Flux of BC to Parameter Changes in SKYHI[a]

| Station Name | Modeled | | | Measured[b] |
|---|---|---|---|---|
| | Standard | Halved Wet Deposition | Halved Transformation Time | |
| Northern Sweden | 1015–2766 | 585–1590 | 830–1956 | 4000–6000 |
| Southern Sweden | 2299–7198 | 1398–4326 | 2052–6091 | 5000–11000 |
| Seattle | 1890–2045 | 1287–1466 | 2193–2429 | 648–9576 |

[a]Range in the modeled values is the range of the monthly modeled means for the same period as the measurements. All measurements are in micrograms per square meter per month.
[b]*Ogren et al.* [1984].

relative to the standard case. A similar explanation can be made for the flux of aerosol to the surface. With the exception of the two sites in Nova Scotia, halving the wet deposition rate causes the model to move away from the observations. For the two sites in Nova Scotia the wet deposition is still overestimated by a factor of at least 2.

[86] Conversely, one could expect that halving the time for transformation from hydrophobic to hydrophilic aerosol would result in an increase in the wet deposition concentration and flux due to the aerosol being more hydrophilic. In fact, the opposite is true at most sites. At sites that are close to source regions (Gif-sur-Yvette and Seattle) the wet deposition concentration does increase. However, as one moves away from the source regions, the wet deposition concentrations become similar to or less than those in the standard case. As one gets to Arctic latitudes, the wet deposition concentrations are similar to those found when the wet deposition was halved. This behavior can be explained by the aerosol near source regions becoming more hydrophilic and therefore more easily deposited, which increases the wet deposition near the source regions. However, the increased wet deposition near source regions depletes the aerosol in the atmosphere, and the air concentrations are lowered in more remote regions, with the result that the wet deposition there is also decreased. As the measurements are biased toward the Arctic region, where the air concentrations are also underestimated, it is difficult to determine whether the underestimation of the wet deposition in this region is due to excessive wet deposition near the source regions or to lack of transport of aerosol to this region. Wet deposition measurements at lower latitudes where the transport issue is not a problem would further resolve this point. The wet deposition flux (Table 5b) increases at Seattle and decreases in Sweden in a similar fashion to the concentration data.

## 5. Conclusions

### 5.1. Observations and Model Simulations

[87] A systematic series of SKYHI GCM integrations reveals the considerable sensitivity of the simulated BC and OC concentrations to aerosol physical parameters and to meteorological conditions (partitioning of the emissions into hydrophobic and hydrophilic varieties, transformation rate from hydrophobic and hydrophilic, wet deposition process, and intensity and frequency of precipitation). Temporal variability of concentrations affects interpretation of both simulation and observations. In several instances the variability in measured concentrations is very large. All of the above factors affect the rigor of evaluation of the model simulations and, more particularly, affect the comparison with the available observations.

[88] The simulations of surface concentrations of BC and OC aerosols are in reasonable agreement with the available measured concentrations to within about a factor of 2 at a majority of the sites. Areas with large concentrations, namely, near source regions, are better simulated; however, in remote regions the model tends to underestimate the measured concentrations, which may be due to excessive scavenging and weaker transport to remote regions from source regions. A secondary factor likely is accuracy of the hydrophobic and hydrophilic carbonaceous aerosol emissions data used. In the case of the OC aerosol the model underestimates the surface concentrations, although the number of measurements in regions other than the United States is limited.

[89] The atmospheric burdens of the carbonaceous aerosol simulated by the SKYHI model and studied here are lower than in previous studies. The atmospheric burden of the aerosol is dominated by the concentrations near the surface. Because of this factor and the model-observation comparisons of surface concentrations (Figure 8) it is inferred that the model tends to overestimate the BC burden in rural areas and underestimate it in remote regions (see Figure 8). The product of the area of remote regions and the model underestimation of the atmospheric concentrations in remote regions emphasize that the burden found here may be a lower limit for the global mean atmospheric burden of BC among model simulations to date. Likewise, the global mean atmospheric burden of OC is also underestimated. However, the vertical distribution of the BC aerosol suggests that the burden of BC in the middle to upper troposphere is overestimated. The implication of too much BC in the upper troposphere is that some other sink needs to be applied to this aerosol type.

[90] An important factor that affects the interpretation of the model observation comparisons is the quality and availability of the measurements. The observations do not span the globe or even all the land masses and certainly are sparse in terms of height profiles. Further, the observations do not cover all the seasons at most sites. Even more, there is an absence of long-term continuous measurements (say, 5 years or more), and there are significant gaps in time series. Because of the short lifetimes of the aerosols (<7 days) the space-time inhomogeneous distribution of the aerosol is incapable of being fully understood in the absence of comprehensive measurement strategies, thus rendering quantitative evaluations of model-observation differences somewhat tentative at this stage. While the above is symptomatic for most aerosol types at present, BC and OC raise additional problems in that they are difficult to characterize and the techniques to infer their concentrations are not fully reliable, contributing another source of uncertainty. Nevertheless, given the variability present in the available observations, the model results indicate that the simulated concentrations of BC and OC tend to be within about a factor of 2 of the observations at a majority of the sites.

[91] The paucity of data to compare with is troubling. There are very few measurement sites in fossil fuel aerosol dominated regions. Of these, Mauna Loa and Mace Head have the longest records, with 8 years of data, which is a reasonable length of record. The other two sites where a detailed comparison is made have a record of only 4 years. In order to evaluate the interannual variation of the concentration of BC and OC, 4 years of daily observations is at the very lowest limit of a record that can be used for analyses. A record of at least a decade is probably the minimum that is necessary, especially if the geometric deviation of the measurements is required.

[92] The model runs show significant interannual variability in the monthly mean BC and OC concentrations. This shows the necessity of both multiyear model runs and multiyear observations. While short-term observation campaigns are useful in that they provide some information on

the possible magnitude of the aerosol concentration, they do not provide a measurement that one can have confidence in as a long-term average.

[93] For a robust evaluation of any model, a comparison of many long-term measurements at stations distributed around the globe is needed. At present the long-term measurement sites are located in the United States and western Europe. While a number of short-term measurements have been compared with this model (section 3.2.2), the short-term nature of these measurements does not guarantee that they are representative of the long-term mean. As was shown in section 3.1, the geometric deviation of a distribution of daily mean observations is greater than that for monthly mean, with the probability of having an observation that is significantly different from the true long-term mean being higher.

[94] From the general circulation model perspective the biggest source of uncertainty is the simulation of the frequency and intensity of precipitation of each grid point, followed by potential biases in the 3-D winds. Other possible sources of uncertainty include the height profile of the precipitation formation, which we assume is constant, the use of constant liquid water contents, and the possibility that the precipitation is being attributed to convective processes rather than to stratiform processes. The use of a larger liquid water content for convective processes could lead to a reduction in the deposition flux by a factor of 4. Despite the numerous possible sources of uncertainty, this study suggests that the frequency and intensity of the precipitation are probably the most important sources of uncertainty in the wet deposition scheme. Despite the deficiencies identified in the measurements and in the atmospheric and aerosol modeling, the extensive sensitivity integrations suggest that, given the variability and uncertainty elements, the results are in reasonable agreement with the observations.

### 5.2. Sensitivity Studies

[95] A major part of this work is the number of sensitivity studies involved. All of the significant parameters in the carbon aerosol model are examined in order to test the significance of their variation on the global burden of aerosol. In each case the column burden and zonal mean concentration were changed in a statistically significant manner over at least a portion of the globe. The magnitude of these changes was different for the different tests, however. Of the sensitivity tests that were performed here for the global mean column burden, the wet deposition scheme is the most sensitive parameter when dealing with carbonaceous aerosol, followed by the transformation time for the conversion of hydrophobic to hydrophilic aerosol. The partition of the emissions between the hydrophobic and hydrophilic components appears to have the least significant effect for the tests performed. However, when dealing with more localized domains such as individual measurement sites or the seasonal cycle in regions, distinguishing between the relative importance of these processes, along with the issue of meteorological variability, becomes difficult, in general.

[96] In some of the sensitivity studies, certain regions do not show a statistically significant change. Eastern Europe, China, India, southern Brazil, and, to a lesser extent, western Europe and the United States show no significant change in column burden when the transformation time is doubled or when the emissions are more hydrophobic than in the standard case. However, in more remote regions of the globe, especially Antarctica, the variability is less, so the change in the mean is much more statistically significant. It would therefore appear that modeling the carbonaceous aerosol and elucidating which of the parameters is the primary factor in determining the lifetime of the carbonaceous aerosol would benefit from long-term measurements made in more remote regions.

[97] The sensitivity studies in the vertical profiles indicate that the zonal mean is most sensitive to changes in the aerosol model in the region between 60° and 90° of each hemisphere at the 500-hPa level. While modeling the mean aerosol concentration correctly is probably the most important test of the model, the variability of the model concentrations is an essential component and should also be included in any evaluation of the model.

[98] Further improvement toward a better understanding of atmospheric concentrations of BC and OC requires a more reliable (1) observational database of not only the means but also variability, at least on synoptic timescales over long time periods (at least a decade); (2) knowledge of aerosol physical characteristics, for example, aging, hydrophilic nature, and secondary OC sources; (3) observation of intensity and frequency of precipitation (at least on a daily basis); and (4) robust model simulation of the tropospheric meteorology, including winds and rainfall.

## Appendix A: Black Carbon Site Measurement Sites as Referred to in Figure 8

A: 1 SaNic: Saint Nicholas Island
2 SwUsa: South west United States
3 ARCH1: Arches National Park
4 BRCA1: Bryce Canyon National Park
5 CANY1: Canyonlands National Park
6 CHIR1: Chiricahua National Monument
7 GRCA1: Grand Canyon National Park
8 LOPE1: Lone Peak Wilderness
9 MEAD1: Meadview, Arizona
10 PEFO1: Petrified Forest National Park
11 SAGU1: Saguaro National Monument
12 SYCA1: Sycamore Canyon Arizona
13 TONT1: Tonto National Monument

B: 1 mtgib: Mt Gibbs, North Carolina
2 hlfax: Halifax, Nova Scotia
3 Allgh: Allegheny Mountain, Pennsylvania
4 Chebo: Cheboque Point, Nova Scotia
5 ACAD1: Acadia National Park
6 DOSO1: Dolly Sods Wilderness, West Virginia
7 GRSM1: Great Smoky Mountains National Park
8 JEFF1: Jefferson National Forest
9 LYBR1: Lye Brook Wilderness, Vermont
10 MACA1: Mammoth Cave National Park
11 MOOS1: Moosehorn National Wildlife Refuge
12 SHEN1: Shenandoah National Park
13 SHRO1: Shining Rock Wilderness

C: 1 jungf: Jungfraujoch, Switzerland
2 wport: Western Portugal
3 Corse: Corsica

4 Lande: Landes, France
5 ClerF: Clermont Ferrand, France
6 Orlea: Orleans, France
7 Hemsb: Hemsby, England
8 Peten: Peten, Netherlands
D: 1 sanpc: San Pietro Capofiume, Italy
2 Rorvi: Rorvik, Sweden
3 KapAr: Kap Arkona, Germany
4 Kurre: Kurresare, Estonia
5 Boist: Böisto Island, Finland
E: 1 cheju: Cheju Island, South Korea
2 Chici: Chici Island, Japan
3 Hachi: Hachi Island, Japan
4 OkiIs: Oki Island, Japan
5 WstMt: West Mountain, China
F: 1 Sarga: Sargasso Sea
2 Bermu: Bermuda
3 Abast: Abastumani, Georgia
4 Kislo: Kislovodsk
5 Abisk: Abisko, Sweden
6 Gland: Summit, Greenland
7 NyAle: Ny Alesund, Spitzbergen
8 EstAr: East Arctic
9 Enewe: Enewetak
10 Ferna: Fernando do Noronha

## Appendix B: Organic Carbon Site Measurement Sites as Referred to in Figure 12

A: 1 SaNic: Saint Nicholas Island
2 ARCH1: Arches National Park
3 CANY1: Canyonlands National Park
4 CHIR1: Chiricahua National Monument
5 GRCA1: Grand Canyon National Park
6 LOPE1: Lone Peak Wilderness
7 MEAD1: Meadview, Arizona
8 PEFO1: Petrified Forest National Park
9 SAGU1: Saguaro National Monument
10 SYCA1: Sycamore Canyon Arizona
11 TONT1: Tonto National Monument
B: 1 Allgh: Allegheny Mountain, Pennsylvania
2 ACAD1: Acadia National Park
3 DOSO1: Dolly Sods Wilderness West Virginia
4 GRSM1: Great Smoky Mountains National Park
5 JEFF1: Jefferson National Forest
6 LYBR1: Lye Brook Wilderness, Vermont
7 MACA1: Mammoth Cave National Park
8 MOOS1: Moosehorn National Wildlife Refuge
9 SHEN1: Shenandoah National Park
10 SHRO1: Shining Rock Wilderness
C: 1 wport: Western Portugal
2 Corse: Corsica
3 Lande: Landes, France
4 Peten: Peten, Netherlands
D: 1 sanpc: San Pietro Capofiume, Italy
2 Rorvi: Rorvik, Sweden
E: 1 cheju: Cheju Island, South Korea
2 Chici: Chici Island, Japan
3 Hachi: Hachi Island, Japan
4 OkiIs: Oki Island, Japan
F: 1 Sarga: Sargasso Sea
2 Bermu: Bermuda
3 Abast: Abastumani, Georgia
4 Gland: Summit, Greenland
5 Enewe: Enewetak

[99] **Acknowledgments.** We would like to acknowledge the ECMWF for the data, Joyce Harriss for providing the trajectory data for the CMDL sites, and J. Ogren and the Climate Monitoring and Diagnostics Laboratory aerosol group for use of the absorption data from the CMDL sites. We would also like to thank R. S. Hemler for his help with the SKYHI model and W. J. Moxim for the back-trajectory program for the SKYHI model. This work was funded by the National Atmospheric and Oceanic Administration (grant NA76GP0350).

## References

Andreae, M. O., T. W. Andreae, R. J. Ferek, and H. Raemdonck, Long-range transport of soot carbon in the marine atmosphere, *Sci. Total Environ.*, *36*, 73–80, 1984.

Bahrmann, C. P., and V. K. Saxena, Influence of air mass history on black carbon concentrations and regional climate forcing in southeastern United States, *J. Geophys. Res.*, *103*, 23,153–23,161, 1998.

Balkanski, Y., Atmospheric residence times of continental aerosols, Ph.D. thesis, Harvard Univ., Cambridge, Mass., 1991.

Berner, A., S. Sidla, Z. Galambos, C. Kruisz, R. Hitzenberger, H. M. ten Brink, and G. P. A. Kos, Modal character of atmospheric black carbon size distributions, *J. Geophys. Res.*, *101*, 19,559–19,565, 1996.

Blake, D. F., and K. Kato, Latitudinal distribution of black carbon soot in the upper troposphere and lower stratosphere, *J. Geophys. Res.*, *100*, 7195–7202, 1995.

Brorström-Lundén, E., and G. Lovblad, Deposition of soot related hydrocarbons during long-range transport of pollution to Sweden, *Atmos. Environ., Part A*, *25*, 2251–2257, 1991.

Brorström-Lundén, E., A. Lindskog, and J. Mowrer, Concentrations and fluxes of organic compounds in the atmosphere of the Swedish west coast, *Atmos. Environ.*, *28*, 3605–3615, 1994.

Cachier, H., Carbonaceous combustion particles, in *Atmospheric Particles*, edited by R. M. Harrison and R. E. Van Grieken, pp. 295–348, John Wiley, New York, 1998.

Cachier, H., M.-P. Brémond, and P. Buat-Ménard, Carbonaceous aerosols from different tropical biomass burning sources, *Nature*, *340*, 371–373, 1989a.

Cachier, H., M.-P. Brémond, and P. Buat-Ménard, Determination of atmospheric soot carbon with a simple thermal method, *Tellus, Ser. B*, *41*, 379–390, 1989b.

Cachier, H., M.-P. Brémond, and P. Buat-Ménard, Organic and black carbon aerosols over marine regions of the Northern Hemisphere, in *Proceedings of the International Conference on Atmospheric Chemistry*, edited by L. Newman, W. Wang, and C.S. Kiang, pp. 249–261, Brookhaven Natl. Lab., Upton, N.Y., 1990.

Castro, L. M., C. A. Pio, R. M. Harrison, and D. J. T. Smith, Carbonaceous aerosol in urban and rural European atmospheres: Estimation of secondary organic carbon concentrations, *Atmos. Environ.*, *33*, 2771–2781, 1999.

Chýlek, P., et al., Black carbon: Atmospheric concentrations and cloud water content measurements over southern Nova Scotia, *J. Geophys. Res.*, *101*, 29,105–29,110, 1996.

Chýlek, P., L. Kou, B. Johnson, F. Boudala, and G. Lesins, Black carbon concentrations in precipitation and near surface air in and near Halifax, Nova Scotia, *Atmos. Environ.*, *33*, 2269–2277, 1999.

Clarke, A. D., and K. J. Noone, Soot in the Arctic snowpack: A cause for perturbations in radiative transfer, *Atmos. Environ.*, *19*, 2045–2053, 1985.

Cooke, W. F., and J. J. N. Wilson, A global black carbon aerosol model, *J. Geophys. Res.*, *101*, 19,395–19,409, 1996.

Cooke, W. F., S. G. Jennings, and T. G. Spain, Black carbon measurements at Mace Head, 1989–1996, *J. Geophys. Res.*, *102*, 25,339–25,346, 1997.

Cooke, W. F., C. Liousse, H. Cachier, and J. Feichter, Construction of a $1° \times 1°$ fossil fuel emission data set for carbonaceous aerosol and implementation and radiative impact in the ECHAM-4 model, *J. Geophys. Res.*, *104*, 22,137–22,162, 1999.

Ducret, J., and H. Cachier, Particulate carbon content in rain at various temperate and tropical locations, *J. Atmos. Chem.*, *15*, 55–67, 1992.

Fels, S. B., J. D. Mahlman, M. D. Schwarzkopf, and R. W. Sinclair, Stratospheric sensitivity to perturbations in ozone and carbon dioxide: Radiative and dynamical responses, *J. Atmos. Sci.*, *37*, 2265–2297, 1980.

Ganzeveld, L., J. Lelieveld, and G.-J. Roelofs, A dry deposition parameterization for sulfur oxides in a chemistry and general circulation model, *J. Geophys. Res.*, *103*, 5679–5694, 1998.

Hamilton, K., R. J. Wilson, J. D. Mahlman, and L. J. Umscheid, Climatology of the SKYHI troposphere-stratosphere-mesosphere general circulation model, *J. Atmos. Sci.*, *52*, 5–43, 1995.

Hansen, A. D. A., and T. Novakov, Aerosol black carbon measurements over the western Atlantic Ocean, *Global Biogeochem. Cycles*, *2*, 41–45, 1988.

Haywood, J. M., and V. Ramaswamy, Global sensitivity studies of the direct radiative forcing due to anthropogenic sulfate and black carbon aerosols, *J. Geophys. Res.*, *103*, 6043–6058, 1998.

Hegg, D. A., J. Livingston, P. V. Hobbs, T. Novakov, and P. Russell, Chemical apportionment of aerosol column optical depth off the mid-Atlantic coast of the United States, *J. Geophys. Res.*, *102*, 25,293–25,303, 1997.

Heintzenberg, J., Size-segregated measurements of particulate elemental carbon and aerosol light absorption at remote Arctic locations, *Atmos. Environ.*, *16*, 2461–2469, 1982.

Heintzenberg, J., R. J. Charlson, A. D. Clarke, C. Liousse, V. Ramaswamy, K. P. Shine, M. Wendisch, and G. Helas, Measurements and modelling of aerosol single-scattering albedo: Progress, problems and prospects, *Beitr. Phys. Atmos.*, *70*, 249–263, 1997.

Hidy, G. M., P. K. Mueller, H. H. Wang, J. Karney, S. Twiss, M. Imada, and A. Alcocer, Observations of aerosols over southern California coastal waters, *J. Appl. Meteorol.*, *13*, 96–107, 1974.

Hoffman, E. J., and R. A. Duce, Organic carbon in marine atmospheric particulate matter: Concentration and particle size distribution, *Geophys. Res. Lett.*, *4*, 449–452, 1977.

Holloway, J. L., and S. Manabe, Simulation of climate by a global general circulation model, I, Hydrological cycle and heat balance, *Mon. Weather Rev.*, *99*, 335–370, 1971.

Keeler, G. J., S. M. Japar, W. W. Brachaczek, R. A. Gorse, J. M. Norbeck, and W. R. Pierson, The sources of aerosol elemental carbon at Allegheny Mountain, *Atmos. Environ., Part A*, *24*, 2795–2805, 1990.

Kim, Y. P., K. C. Moon, J. H. Lee, and N. J. Baik, Concentrations of carbonaceous species in particles at Seoul and Cheju in Korea, *Atmos. Environ.*, *33*, 2751–2758, 1999.

Lacis, A. A., and J. E. Hansen, A parameterisation for the absorption of solar radiation in the Earth's atmosphere, *J. Atmos. Sci.*, *31*, 118–132, 1974.

Lavanchy, V. M. H., H. W. Gaggeler, S. Nyeki, and U. Baltensperger, Elemental carbon (EC) and black carbon (BC) measurements with a thermal method and an aethalometer at the high-alpine research station Jungfraujoch, *Atmos. Environ.*, *33*, 2759–2769, 1999.

Lin, S. J., and R. B. Rood, Multidimensional flux-form semi-Lagrangian transport schemes, *Mon. Weather Rev.*, *124*, 2046–2070, 1996.

Liousse, C., H. Cachier, and S. G. Jennings, Optical and thermal measurements of black carbon aerosol content in different environments: Variation of the specific attenuation cross section, σ, *Atmos. Environ., Part A*, *27*, 1203–1211, 1993.

Liousse, C., J. E. Penner, C. Chuang, J. J. Walton, H. Eddleman, and H. Cachier, A global three-dimensional model study of carbonaceous aerosols, *J. Geophys. Res.*, *101*, 19,411–19,432, 1996.

Lyubovtseva, Y. S., and L. G. Yatskovich, Soot in the aerosols of different regions, *J. Aerosol Sci.*, *20*, 1269–1272, 1989.

Mahlman, J. D., J. P. Pinto, and L. J. Umscheid, Transport, radiative, and dynamical effects of the Antarctic ozone hole: A GFDL "SKYHI" model experiment, *J. Atmos. Sci.*, *51*, 489–508, 1994.

Malm, W. C., J. F. Sisler, D. Huffman, R. A. Eldred, and T. A. Cahill, Spatial and seasonal trends in particle concentration and optical extinction in the United States, *J. Geophys. Res.*, *99*, 1347–1370, 1994.

Masclet, P., V. Hoyau, J. L. Jaffrezo, and H. Cachier, Polycyclic aromatic hydrocarbon deposition on the ice sheet of Greenland, I, Superficial snow, *Atmos. Environ.*, *34*, 3195–3207, 2000.

Mukai, H., Y. Ambe, K. Shibata, T. Muku, K. Takeshita, T. Fukuma, J. Takahashi, and S. Mizota, Long-term variation of chemical composition of atmospheric aerosol on the Oki Islands in the Sea of Japan, *Atmos. Environ., Part A*, *24*, 1379–1390, 1990.

Noone, K. J., and A. D. Clarke, Soot scavenging measurements in Arctic snowfall, *Atmos. Environ.*, *22*, 2773–2778, 1988.

Novakov, T., and C. E. Corrigan, Cloud condensation nucleus activity of the organic component of biomass smoke particles, *Geophys. Res. Lett.*, *23*, 2141–2144, 1996.

Ogren, J. A., P. J. Groblicki, and R. J. Charlson, Measurement of the removal rate of elemental carbon from the atmosphere, *Sci. Total Environ.*, *36*, 329–338, 1984.

Ohta, S., and T. Okita, Measurements of particulate carbon in urban and marine air in Japanese areas, *Atmos. Environ.*, *18*, 2439–2445, 1984.

Parungo, F., C. Nagamoto, M.-Y. Zhou, A. D. A. Hansen, and J. Harris, Aeolian transport of aerosol black carbon from China to the ocean, *Atmos. Environ.*, *28*, 3251–3260, 1994.

Penner, J. E., R. C. Easter, and S. J. Ghan, A parameterization of cloud droplet nucleation, II, Multiple aerosol types, *Atmos. Res.*, *36*, 39, 1995.

Pertuisot, M. H., Transfert du carbone atmosphérique dans les neiges et les pluies, Ph.D. thesis, Denis Diderot Univ., Paris, 1997.

Pinnick, R. G., G. Fernandez, E. Martinez-Andazola, B. D. Hind, A. D. A. Hansen, and K. Fuller, Aerosol in the arid southwestern United States: Measurements of mass loading, volatility, size distribution, absorption characteristics, black carbon content, and vertical structure to 7 km above sea level, *J. Geophys. Res.*, *98*, 2651–2666, 1993.

Polissar, A. V., Measurements of the soot mass concentration and particle-size distribution of atmospheric aerosol in the eastern Arctic. *Izv. Russ*, *Acad. Sci. Atmos. Oceanic Phys., Engl. Transl.*, *29*, 66–73, 1993.

Pueschel, R. F., D. F. Blake, K. G. Snetsinger, A. D. A. Hansen, S. Verma, and K. Kato, Black carbon (soot) aerosol in the lower stratosphere and upper troposphere, *Geophys. Res. Lett.*, *19*, 1659–1662, 1992.

Ramachandran, S., V. Ramaswamy, G. L. Stenchikov, and A. Robock, Radiative impact of the Mount Pinatubo volcanic eruption: Lower stratospheric response, *J. Geophys. Res.*, *105*, 24,409–24,429, 2000.

Ramaswamy, V., and S. M. Friedenreich, A study of broadband parameterizations of the solar radiative interactions with water vapor and water drops, *J. Geophys. Res.*, *97*, 11,487–11,512, 1992.

Raunemaa, T., K. Kuuspalo, T. Alander, E. Tamm, A. Mirme, and V. Laine, Black carbon and aerosol in Böisto Island, *J. Aerosol Sci.*, *24*, S29–S30, 1993.

Schwarzkopf, M. D., and S. B. Fels, The simplified exchange method revisited: An accurate, rapid method for computation of infrared cooling rates and fluxes, *J. Geophys. Res.*, *96*, 9075–9096, 1991.

Schwarzkopf, M. D., and V. Ramaswamy, Radiative effects of $CH_4$, $N_2O$, halocarbons, and the foreign-broadened $H_2O$ continuum: A GCM experiment, *J. Geophys. Res.*, *104*, 9467–9488, 1999.

Smith, D. M., M. S. Akhter, J. A. Jassim, C. A. Sergides, W. F. Welch, and A. R. Chughtai, Studies of the structure and reactivity of soot, *Aerosol Sci. Technol.*, *10*, 311–325, 1989.

Wetherald, R. T., and S. Manabe, Cloud feedback processes in a general circulation model, *J. Atmos. Sci.*, *45*, 1397–1415, 1988.

Wolff, G. T., M. S. Ruthkosky, D. P. Stroup, P. E. Korsog, M. A. Ferman, G. J. Wendel, and D. H. Stedman, Measurements of $SO_x$, $NO_x$ and aerosol species on Bermuda, *Atmos. Environ.*, *20*, 1229–1239, 1986.

Zappoli, S., et al., Inorganic, organic and macromolecular components of fine aerosol in different areas of Europe in relation to their water solubility, *Atmos. Environ.*, *33*, 2733–2743, 1999.

---

W. F. Cooke and V. Ramaswamy, Geophysical Fluid Dynamics Laboratory, P.O. Box 308, Forrestal Campus, Princeton, NJ 08542-0308, USA. (wfc@gfdl.noaa.gov; vr@gfdl.noaa.gov)

P. Kasibhatla, Nicholas School of the Environment, Duke University, Box 90328, Durham, NC 27708-0328, USA. (prasad@pinus.Env.Duke.Edu)